Reviewed Preprint
v1 • October 1, 2025
Not revised

Reviewed Preprint
v2 • June 3, 2026
Revised by authors

For correspondence:
anna.c.schneider@uni-kassel.de

* These authors contributed equally

Competing interests: Conflict of interest: Authors report no conflict of interests.

Funding: See page 30

Reviewing editor: John Ewer, Universidad de Valparaiso, Chile

Orco regulates the circadian activity of pheromone-sensitive olfactory receptor neurons in hawkmoths

Aditi Vijayan*,1, Mauro Forlino*,2, Yajun Chang[1], Pablo Rojas[2], Katrin Schröder[1], Anna C Schneider[1], Martin E Garcia[2], Monika Stengl[1]

[1]Animal Physiology and Center for Interdisciplinary Nanostructure Science and Technology, FB 10, University of Kassel, Kassel, Germany • [2]Theoretical Physics and Center for Interdisciplinary Nanostructure Science and Technology, FB10, University of Kassel, Kassel, Germany

eLife Assessment

This **valuable** study uses technically **compelling** long-term in vivo recordings and computational modeling to investigate whether hawkmoth olfactory receptor neurons show circadian modulation of spontaneous firing. The authors further propose the provocative model that post-translational mechanisms, rather than the transcriptional-translational processes, may contribute to circadian regulation of neuronal excitability. However, the evidence for circadian firing in these neurons, and for post-translational modification of Orco as the underlying mechanism, remains **incomplete**. In contrast, the study does provide strong evidence that the application of cyclic nucleotides can modulate Orco-dependent activity at a single time point, and reports that the temporal pattern of Orco transcript abundance is not circadian.

https://doi.org/10.7554/eLife.108100.2.sa2

Abstract

The mating behavior of nocturnal *Manduca sexta* hawkmoths is under strict temporal control. It is orchestrated via circadian and ultradian oscillations in sex-pheromone stimuli as social zeitgeber. The extremely sensitive pheromone-detecting olfactory receptor neurons (ORNs) that innervate the long trichoid sensilla on the male's antennae are peripheral circadian clocks. They express the transcriptional-translational feedback loop (TTFL) circadian clockwork, best characterized in *Drosophila melanogaster*. In hawkmoths, it is still unknown whether or how the ORN TTFL clockwork regulates the daily rhythms in pheromone sensitivity and in temporal resolution of ultradian pheromone pulses as prerequisites to the temporal regulation of hawkmoth mating behavior.

We hypothesize that, rather than the slow TTFL clock, a more rapidly adaptive post-translational feedback loop (PTFL) clockwork, associated with the ORN plasma membrane, allows for temporal control of pheromone detection via generation of multiscale endogenous membrane potential oscillations. The potential oscillations of the PTFL clock could rapidly synchronize to oscillations of pheromone stimuli at different timescales, thus enabling the prediction of stimulus patterns as a mechanism for active sensing. With *in vivo* long-term tip recordings of long trichoid sensilla of male hawkmoths, we analyzed the spontaneous spiking activity indicative of the ORNs' endogenous membrane potential oscillations. Consistent with our hypothesis of a multiscale PTFL clock in hawkmoth ORNs, spontaneous spiking was modulated on ultradian and circadian timescales, with maximum activity at night. When we blocked the evolutionarily conserved olfactory receptor coreceptor (Orco), the circadian modulation was abolished but the ultradian frequency modulation of the spontaneous activity remained. Consistent with PTFL control, Orco was not under the transcriptional control of the TTFL clock, but its modulation was dependent on

cAMP. We could replicate the experimental data in a conductance-based computational model of an ORN. In this model, Orco conductivity changed as a function of fluctuating 2nd messenger levels. This study demonstrates that a PTFL clock is sufficient to impose a circadian pattern on ORN sensitivity.

Significance statement

It is generally assumed that all circadian rhythms in an organism are driven by a transcriptional-translational feedback loop (TTFL) clock. In this study, we demonstrate with *in vivo* recordings of hawkmoth pheromone-sensitive olfactory receptor neurons (ORNs) that the olfactory receptor coreceptor (Orco) is the key pacemaker channel for controlling circadian, but not all ultradian, rhythms in spontaneous spiking activity. Since Orco expression is not driven by the TTFL clock, its conductance appears to be controlled by a post-translational feedback loop (PTFL) membrane clock via 2nd messengers. Accordingly, our computational model suggests that ORN sensitivity is tuned by periodic changes in the conductivity of an Orco ion channel, which is mediated by cycling levels of cyclic nucleotides. This highlights the role of the contribution of posttranslational modifications to the generation of circadian rhythmicity.

Introduction

Biological clocks generate endogenous physiological and behavioral oscillations on multiple timescales that persist in the absence of any external timing cues under constant conditions (Lamont and Amir, 2010). Such clocks are essential to generate internal rhythms and to permit their synchronization to external zeitgebers at timescales from milliseconds to years. These synchronized endogenous multiscale clocks thus provide both a continuous time frame for physiology and behavior - the organism's "present time" - and enable organisms to predict and respond to regular, periodic environmental changes (Stengl and Schneider, 2024). Even though endogenous clocks are widespread in prokaryotes and eukaryotes (Géron et al., 2024; Hall and Rosbash, 1993; Millar, 2016; Thaiss et al., 2014), current knowledge about how multiscale clocks are linked over widely diverging timescales remains sparse.

Insect circadian clock neurons, which are tightly connected to visual brain circuits, are amongst the best studied biological clocks (Hall and Rosbash, 1993; Nishiitsutsuji-Uwo and Pittendrigh, 1968; Reinhard et al., 2024). They regulate physiological and behavioral oscillations that underly sleep-wake rhythms tied to the 24 h light-dark cycles on Earth (Dubowy and Sehgal, 2017). Circadian clock neurons possess a molecular clockwork of transcriptional-translational feedback loops (TTFLs). This TTFL clock generates endogenous oscillations of clock gene mRNA and protein levels with a cycle period of ~24 h via negative feedback by proteins that inhibit their own transcription (Hardin, 2011). It is assumed for both insects and mammals that this TTFL comprises the master clockwork that regulates all physiological and behavioral rhythms in the circadian time range through genetically controlled output pathways (Hastings et al., 2020).

Molecular TTFL clockworks were not only found in central brain clock neurons but also in sensory neurons, such as olfactory receptor neurons (ORNs) in insect antennae, where they play a role in odor-dependent circadian behaviors like feeding, pollination, reproduction, and navigation (Flecke et al., 2010; Flecke and Stengl, 2009; Krishnan et al., 1999; Merlin et al., 2009, 2006; Page and Koelling, 2003; Plautz et al., 1997; Sauman and Reppert, 1998; Schendzielorz et al., 2015; Schuckel et al., 2007; Tanoue et al., 2004; Zhou et al., 2005). Little is known about how the TTFL clockwork of insect ORNs regulates circadian rhythms in chemosensory sensitivity that underlie the circadian control of these different behaviors.

At night, male nocturnal *Manduca sexta* hawkmoths are very sensitive to the sex pheromone blend that their conspecific females release in an intermittent pattern (Itagaki and Conner, 1988). The intermittency is a prerequisite to maintain the male's search flight, which is suspended at pulse frequencies >30 Hz (Baker et al., 1985; Baker and Vogt, 1988; Stengl, 2010). The pheromone pulses are resolved of up to 3 Hz by pheromone-specific ORNs in the antenna's long trichoid sensilla (Lee and Strausfeld, 1990; Marion-Poll and Tobin, 1992).

Pheromone-specificity is provided by odor receptor (OR) subunits in the ciliary membranes of ORNs that heteromerize with the conserved olfactory receptor co-receptor Orco (Nakagawa and Vosshall, 2009; Stengl and Funk, 2013; Wicher and Miazzi, 2021). The insect odor transduction cascade is still under debate and seems to involve both ionotropic and metabotropic pathways (Sato et al., 2008; Schneider et al., 2025; Wicher et al., 2008). While there is no general agreement on the role of Orco, it is known that in heterologous expression systems Orco homo- and heteromers form a slow, leaky, non-specific cation channel, which depolarizes the cells (Jones et al., 2011; Sargsyan et al., 2011; Sato et al., 2008; Wicher, 2018; Wicher et al., 2008). *In vivo* tip recordings of long trichoid sensilla in *M. sexta* confirmed that Orco acts as leaky cation channel, acting as a pacemaker channel, because it promotes ultradian membrane potential oscillations that underly the spontaneous action potential activity (Nolte et al., 2013). These potential oscillations turn the ORNs into ultradian temporal filters that are sensitive to the frequency of the pheromone pulses they encounter. Pheromone pulses that arrive at a similar frequency as the endogenous sub-threshold membrane potential oscillations would synchronize these oscillations and would be more likely to elicit action potential trains. Therefore, this pacemaker channel-dependent mechanism would allow for active sensing if endogenous membrane potential oscillations are in the physiological range that is necessary for tracking intermittent pheromone pulses.

It is not known whether the Orco-dependent membrane potential oscillations also occur at circadian timescales, and whether or how they are linked to ultradian potential oscillations. One hypothesis is that the molecular TTFL clockwork of ORNs exclusively controls endogenous circadian rhythms of the membrane potential via circadian expression of pacemaker channels like Orco. Alternatively, the plasma membrane of ORNs could by itself constitute an autonomous clock that is entrained by but does not rely on the TTFL clock. Constant levels of ion channels that do not require daily degradation and daily transcription via the TTFL clock, but with modulation of open-time probability by posttranslational modifications, would constitute a more economical and faster adjustable mechanism to generate endogenous membrane potential oscillations (Stengl and Schneider, 2024). This would facilitate active sensing by rapidly tuning odorant/pheromone detection to behaviorally relevant zeitgeber signals in the insect's environment.

Here, we performed a combination of experimental and computational modeling studies to investigate whether Orco plays a role in active sensing at the circadian and/or ultradian timescale via generation of endogenous membrane potential oscillations. We hypothesize that Orco is part of a post-transcriptional feedback loop (PTFL) clockwork in the plasma membrane, rather than being TTFL controlled. To capture naturally occurring, physiologically relevant processes in insect ORNs we performed *in vivo* long-term tip recordings of the spontaneous spiking activity of pheromone-sensitive trichoid sensilla of intact but restrained hawkmoth males.

We corroborated the experimental data with a Hodgkin-Huxley (HH) based computational ORN model. In general, the widely used deterministic HH models do not include circadian control of ion channels. Moreover, the highly dynamic, bursting firing patterns of ORNs cannot be described by the traditional deterministic modeling of neuronal activity. This constitutes a drawback because stochasticity plays a crucial role in shaping firing patterns which are influenced not only by external stimuli but also by the inherent noise involved in channel gating. Therefore, to address the above points realistically, we developed a Langevin formulation of the HH model, which explicitly accounts for the noise introduced by the random opening and closing of ion channels and circadian modulation of the Orco channel conductivity. By integrating channel noise, we could explore how circadian regulation of ionic currents contributes to the variability of firing patterns and how this noise interacts with external stimuli to influence olfactory signal processing.

Our model aims to highlight the advantages of using a stochastic framework for modeling the circadian activity of ORNs. The combined experimental and modeling efforts generate a more complete picture and predictions concerning these autonomous processes in sensory neurons, which are required for future exploration of physiologically relevant anticipatory behaviors that are driven by biological clocks.

Methods

Animals

Nocturnal *M. sexta* hawkmoths were bred and raised from eggs in the rearing facility at the University of Kassel. Males and females were separated during pupal stages. Males were housed isolated from the females to avoid exposure to female pheromones. All experiments were performed with adult males reared in a long-day photoperiod (L:D 17:7 h to prevent diapause) at 25 °C with relative humidity of about 55%. Larvae were fed with an artificial diet modified after Bell and Joachim (1976); adult moths could feed on sugar solution with added vitamins (Roth) *ad libitum* (Riffell et al., 2008).

While all animals were exposed to the same lighting regime as zeitgeber to entrain them up until the start of the experiments, we also attempted pheromone exposure as additional circadian zeitgeber to phase-align spontaneous ORN activity in a subset of males (Ghosh et al., 2024). Without allowing direct contact, virgin males were exposed at zeitgeber time (ZT) 16 to females and naturally occurring pheromone blends in closed mating cages for 30 mins. Males were then moved back into isolation before tip recordings (see below) were started at ZT 17 on the same day. Since we focused on spontaneous spiking activity rather than on pheromone-dependent responses and because repetitive or long pheromone exposure changes the composition of 2nd messenger modulated ion channels in ORNs (Gawalek and Stengl, 2018), we did not employ any further pheromone synchronization protocols.

Solutions

Ringer compositions were taken from (Pézier et al., 2007) and contained (in mM): 6.4 KCl, 12 $MgCl_2$, 1 $CaCl_2$, 12 NaCl, 10 HEPES, 340 glucose for hemolymph ringer (HLR) at 450 mosmol/kg, and 172 KCl, 3 $MgCl_2$, 1 $CaCl_2$, 25 NaCl, 10 HEPES, 22.5 glucose for sensillum lymph ringer (SLR) at 475 mosmol/kg, both at pH 6.5.

The Orco antagonist OLC15 (N-(4-butylphenyl)-2-((4-ethyl-5-(2-pyridinyl)-4H-1,2,4-triazol-3-yl)thio)acetamide (Chen and Luetje, 2012); kindly provided by Dr. D. Wicher, Max Planck Institute for Chemical Ecology, Jena, Germany) was dissolved in DMSO to a concentration of 100 mM (stock solution stored at 4-8 °C) before being diluted in SLR to a final concentration of 50 µM to be used within one week (stored at 4 °C). We determined in previous studies that, compared to other Orco antagonists, OLC15 is the most specific (Chen and Luetje, 2012; Nolte et al., 2016, 2013; Pask et al., 2013). It is effective at 50 µM, according to dose-response curves, and dose-dependently antagonizes the action of the Orco agonist VUAA1 in intact hawkmoths (Nolte et al., 2016, 2013). DMSO percentage was 0.05% in the final solution.

The cAMP analog 8-bromo-cAMP acetoxymethyl ester (8-Br-cAMP-AM; Biolog Life Science Institute GmbH & Co. KG) was dissolved in DMSO to a concentration of 10 mM (stock solution stored at -20°C) and diluted to a final concentration of 100 mM in either SLR or SLR + 50 µM OLC15.

Electrophysiology

The spontaneous electrical activity of the unstimulated pheromone-sensitive ORNs in a single long trichoid sensillum was recorded extracellularly as *in vivo* tip recording (Kaissling et al., 1987). 1-2-d-old male *M. sexta* that were raised and entrained to zeitgebers as described above were fixed in a custom-made Teflon holder with adhesive tape. The right antenna used for recordings was oriented with its dorsal surface facing up and immobilized near the base with dental wax (Boxing wax strips, KerrHawe SA). Electrodes (Ag/AgCl wire in a glass pipette filled with SLR for the recording electrode and HLR for the reference electrode) were pulled (DMZ-Universal Puller, Zeitz Instruments) from borosilicate capillaries (OD:1.56mm, ID: 1.17mm, without filament; Science Products) to a tip diameter of about 2 µm. All recordings were made at a distance of 2/3 to 3/4 of the antenna length towards its distal end because pheromone-sensitive long-trichoid sensilla (sensilla trichodea type 1) occur in a characteristic, homogenous pattern along the hawkmoth antenna (Kaissling et al., 1989; Kalinová et al., 2001; Lee and Strausfeld, 1990). Furthermore,

all ORNs in long trichoid sensilla express the same Orco staining pattern (Nolte et al., 2016), share largely overlapping ion channel populations, and obvious differences in the activity of ORNs from different annuli have not been reported (c.f., Dolzer et al., 2003; Gawalek and Stengl, 2018; Schneider et al., 2025). Thus, it is very likely that pheromone encoding mechanisms are not locally restricted along the flagellum. Recording and reference electrodes were located on the same annulus: After cutting off the distal 20 annuli of the antenna with micro scissors, the reference electrode was inserted to a depth of 2 annuli into the antennal lumen from the cut end. The cut was covered with electrode gel (GE Medical Systems Information Technology) to prevent desiccation. Under microscopic control, some tips of the long trichoid sensilla of the annulus were cut off with sharpened Dumont forceps, and the recording electrode was slipped over a single sensillum of an upper sensillar row. Electrodes were moved with manual micromanipulators (MMJ, Märzhäuser Wetzlar; and Leitz, Leica Microsystems) or with motorized micromanipulators (Microstar, Scientifica) with a joystick controller (Scientifica).

ORN activity was amplified 200-fold (custom built amplifier with 10^{12} Ω input impedance, or ELC-01 MX in combination with DPA-2FX, npi, or EXT 10-2F, npi), low pass filtered at 1.3 kHz, digitized at 20 kHz with a Digidata (1550A or 1550B, Molecular Devices), and saved for offline analysis with Clampex 10 (pCLAMP suite, Molecular Devices).

All tip recording experiments were performed at room temperature (21-27 °C) and a relative humidity of 35-60%. These environmental fluctuations across experiments were based on seasonal influences. Throughout each experiment, conditions were stable. To ensure that neither electrode reattachment to the same trichoid sensillum nor application of DMSO influenced spiking activity, we performed two sets of paired experiments at ZT 1-3 in which we recorded the spontaneous activity before and after removing and reattaching the SLR-filled recording electrode to the same sensillum, or recorded the spontaneous activity of the same sensillum in SLR and SLR + 0.15% DMSO. Both treatments did not affect spontaneous spiking activity (Figure 1B).

We recorded ORN activity either in long-day conditions (17:7 LD) or constant darkness (DD) to examine the free-running peripheral ORN clock. For LD experiments, the light regime continued as in the rearing facility during the experiment. For DD and OLC15 experiments, the lights were turned off at the beginning of the recording, i.e., all animals were exposed to the same light zeitgeber until the beginning of the experiment. To examine the effect of Orco on the spontaneous action potential (AP) activity pattern, we used the recording electrode to infuse OLC15 in DD conditions. To examine the effect of cAMP on Orco gating, we recorded the spontaneous ORN activity at the end of the moth's activity phase (ZT 1-3) in SLR as control, and either 8-Br-cAMP-AM, or 8-Br-cAMP-AM + OLC15, infused through the recording electrode.

ORNs generate spontaneous APs. However, high spiking activity during control recordings is indicative of stress, whereas low/no activity could be indicative of damage. Therefore, we only considered experiments in which the average spiking frequency was between 2 Hz and 0.008 Hz in control conditions.

Data analysis

To characterize the spontaneous ORN spiking activity, we first detected spikes with a self-written program in Python. Using the scipy.signal package and find_peaks function, we used a moving mean with 100 samples (5 ms) window size for baseline correction, followed by applying a 8^{th} order low-pass Bessel filter (2000 Hz cutoff frequency) to the raw voltage trace to facilitate spike detection within the following conditions: spike full width (3-15 ms), threshold search for amplitude of spike (0.5-2.5 mV) and threshold prominence (0.1). Two or more consecutive spikes with intervals ≤ 50 ms were considered a burst (Dolzer et al., 2001). We then calculated the following attributes in bins of either 10 min or 1 h for further analysis: instantaneous spike frequency (ISI, 1 / inter-spike interval), inter-burst interval (IBI, time between two consecutive bursts with no single spikes in between), inter-event interval (IEI, time between two events, i.e. two consecutive single spikes, two consecutive bursts, a burst and a consecutive spike, and vice

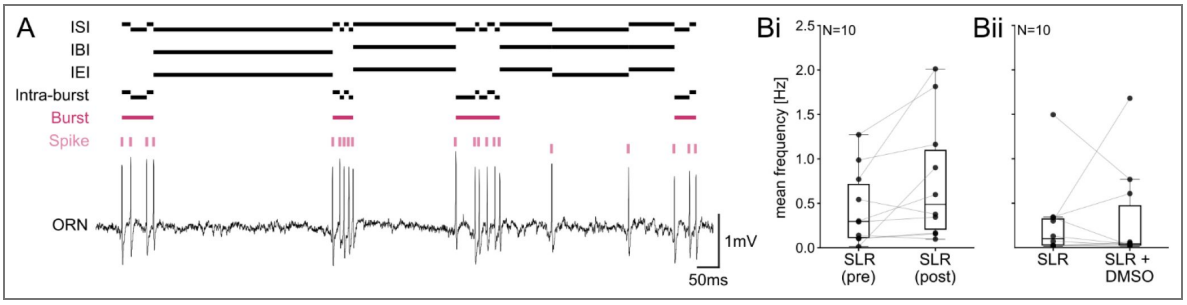

Figure 1. Attributes of pheromone-sensitive ORN spiking patterns.

(**A**) Spikes were identified by their prominence in the raw ORN recording. The inter-spike interval (ISI) was defined as the time from one spike to the next. A train with ≥2 spikes with ISI ≤ 50 ms was considered a burst. The intra-burst interval was the ISIs within a burst, the inter-burst interval (IBI) the ISIs between two bursts, omitting any individual spikes in between. The inter-event interval (IEI) included the ISIs between bursts and individual spikes. Detaching and reattaching the recording electrode to a long trichoid sensillum (**Bi**; paired t-test t(9) = -2.184; p = 0.057; N = 10) or adding DMSO to the SLR (**Bii**; Wilcoxon signed-rank test Z = 0.153; p = 0.922; N = 10) did not affect the mean spiking frequency.

versa), burst duration (time from first to last spike in a burst), percentage of all spikes in the experiment that are members of burst, and mean number of spikes per burst (Figure 1A). All statistics were done with those binned values.

Hawkmoth behavioral and physiological rhythms desynchronize across the population in the absence of zeitgebers like circadian rhythms of pheromone stimulation and daily light-dark cycles. Therefore, we first used RAIN analysis (Thaben and Westermark, 2014) to identify circadian rhythms (24 ± 4 h) in the attributes above for each animal and condition (LD, DD, OLC15) in the 1 h-binned data. Data was downsampled to 2 h resolution and thus included every other 1 h bin to speed up computational time. To further quantify the circadian changes in attributes across animals, it was then necessary to phase align the recordings obtained in DD and OLC15. To achieve this, we used an optimization procedure to calculate the optimal temporal lags for each dataset, aiming to maximize the overall cross-correlation between the calculated binned spike frequency series. The optimization was performed using simulated annealing, which provided a set of time shifts (lags) for each series. These lags were applied to shift the frequency data in a manner that maximized the synchronization between the different subjects' data, resulting in a "subjective ZT" with subjective ZT 0 at the first maximum of the binned ISI for each individual. The objective function used for optimization was the negative sum of pairwise correlations between all series after applying the shifts. The resulting alignment allowed us to compare the frequency patterns across the different conditions.

Once the data were aligned, we computed the mean frequency across all subjects for each bin and each condition. Then, the first high activity period was identified by finding the maximum in the mean frequency series. Subsequently, we identified the second high activity period as the time 24 hours after the first one and the first low activity period was found by locating the minimum in the mean frequency series between the two high activity periods. Besides the mean frequency, we also searched for significant oscillations in IBI, IEI, burst duration, percentage of spikes that are part of bursts, and mean number of spikes per burst. For this we found the maximum value of these statistics within a 3 h range centered in the first low activity period and compared it with the values at the second high activity period.

Continuous wavelet and Fourier analysis were performed using PyBoat (version 0.9.12) (Mönke et al., 2020) to examine the time series of neuronal firing frequency. The continuous wavelet method allows us to detect and characterize rhythmic patterns within the data by identifying frequency components that change over time. Specifically, we used wavelet analysis to determine whether a neuron exhibited circadian and ultradian rhythms. Unlike traditional Fourier analysis, which provides an overall frequency composition but assumes stationarity, wavelet analysis is particularly useful for biological signals because it can reveal how these frequencies evolve dynamically. By applying this approach, we could assess not only the presence of ultradian rhythms but also whether their strength or occurrence fluctuated in a circadian manner, indicating modulation by the 24-hour cycle. For this analysis, we used the 10 min-binned data to have sufficiently high resolution to detect ultradian rhythms. Periods were determined as local maxima in the Fourier power spectra.

Real-time quantitative polymerase chain reaction (qPCR)

We followed the qPCR methodology detailed in (Schneider et al., 2025). Briefly, male moths were isolated and cultured until the second day after eclosion, and the antennae from four individuals were collected every 4 hours for one day, starting at ZT 0, using liquid nitrogen, with four biological replicates per time point. Total RNA was extracted using TRIzol® Reagent (Invitrogen) and quantified for concentration and purity with the NanoDrop ND-1000 spectrophotometer (Thermo Fisher Scientific). First-strand complementary DNA (cDNA) was synthesized using the PrimeScript™ RT reagent Kit with gDNA Erase (Takara Bio Inc.). Primers for *Orco* (F: GCTCGCTACC ACCAAATTGC, R:TCGTGACCCAACTGACAACA; Gene ID: LOC115452348) and for *timeless* (*tim*) (F: TT AAGCCGACCGTAGTGCTG, R: CGTCTTCCGTCCATGTGTCT; Gene ID: LOC115446009) were designed using the Primer-BLAST online program of NCBI. The qPCR was conducted following the protocol

of TB Green® Premix Ex Taq™ II (Tli RNase H Plus) (Takara Bio Inc.), with the program: 95 °C for 30 s, followed by 40 cycles of 95 °C for 5 s, and 60 °C for 30 s. Relative expression levels of *Orco* were calculated using the $2^{-\Delta\Delta Ct}$ method (Livak and Schmittgen, 2001).

Statistics

All statistics were done with self-written python codes, SigmaPlot 12 (Systat Software), or JASP (versions 0.19.03 and 0.95.4, University of Amsterdam) with a significance level $\alpha = 0.05$. Unless noted otherwise, data were checked for normal distribution with Anderson-Darling or Shapiro-Wilk tests and for equal variance with Levene's test. If one of these assumptions failed, we used non-parametric tests, otherwise we used parametric tests.

To assess the statistical significance of observed differences in neuronal activity of the aligned data between ZTs, we applied the Wilcoxon signed-rank test to pairwise comparisons between the first low activity period and the subsequent high activity period and discarded the transient high activity at the beginning of most recordings.

For paired recordings (electrode reattachment, addition of DMSO, or cAMP/cAMP+OLC15 in the same animal, we used either paired student-t test or Wilcoxon signed-rank test, depending on normal distribution of data.

For other data, we used an ANOVA on ranks with either Tukey's or Dunn's post-hoc test for multiple comparisons as indicated.

ORN Model

In this study, we introduce a single-compartment Hodgkin-Huxley (HH) type model of the spontaneous activity of *M. sexta* ORNs (available on GitHub (Forlino et al., 2025)). The model contains 5 sets of ion channels that were previously identified in electrophysiological recordings (Dolzer et al., 2021): the fast sodium (Na^+) and potassium (K^+) channels responsible for the generation of spikes, low voltage-activated calcium channels (LVA) responsible for the initiation of bursts, calcium-gated potassium channels (BK) responsible for the termination of bursts, and the Orco channel, which is a voltage-independent non-specific, cAMP-gated channel. A schematic of the model is provided in Figure 2A. We modeled Orco as a ZT-dependent conductance to represent the effect of the oscillations in cAMP concentration that were identified in both hawkmoth and cockroach antennae (Schendzielorz et al., 2014, 2015, 2012) (Figure 2B, C). For simplicity we chose to use a sine function to directly represent the oscillations in Orco conductivity, but similar results can be achieved by modeling it as an output of a Goodwin model of the circadian clock via cAMP concentration.

Each type of ion channel possesses one or more gates that can open and close individually with transition rates α and β for opening and closing, respectively, of activation gates (n, m) and inactivation gates (h). As a result, each possible combination of open and closed gates defines a possible state in which each ion channel can be found. A schematic of the Markov chain depicting all possible states and transitions for each ion channel is shown in Figure 2D. Each ion channel can conduct current only in the state where all its gates are open.

First, we constructed a deterministic 22-dimensional model to serve as the mean field of the Langevin model following the methodology proposed by Pu and Thomas (2020). Here, one dimension tracks the membrane potential, another the intracellular Ca^{2+} concentration, and the remaining 20 dimensions track the number of channels that are in a specific state of the Markov chains. Considering the conservation of the total number of ion channels, each type of ion channel required one less dimension than the total possible states.

The complete Langevin model adds to the mean field an independent noise source for each transition in the Markov chain. These noise sources are biophysically motivated since the transition between ion channel states is a stochastic process, with the probability of transition determined by the kinetics of each kind of ion channel. The variability in the spiking behavior of a neuron emerges from this non-deterministic gating of individual ion channels. The detailed mathematical description of the model can be found in the Supplementary Material.

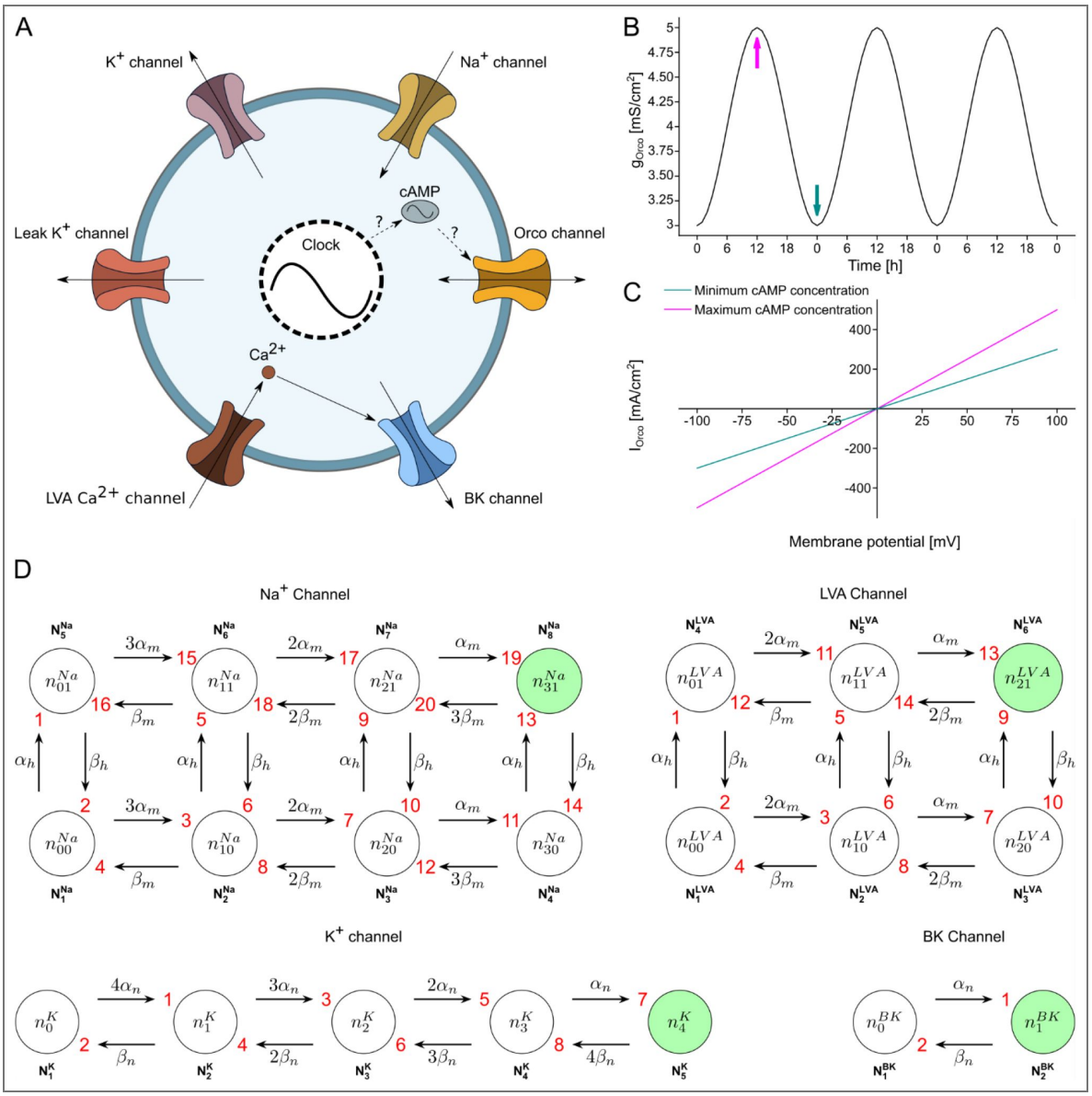

Figure 2. The conductance-based model of a simplified hawkmoth ORN.

(A) Schematic of the model containing a voltage gated sodium channel (Na^+), a voltage gated potassium channel (K^+), a low voltage activated calcium channel (LVA), a calcium and voltage activated potassium channel (BK), a leak channel, and a cAMP-gated leaky non-specific cation channel (Orco). The Orco channel is represented as a linear conductance whose value oscillates with a sinusoidal shape as a function of the ZT. The circadian rhythm in the Orco conductance is hypothesized to result from a cAMP-dependent increase in channel open-time probability (as found in *Drosophila* Orco: (Getahun et al., 2013)) via a circadian oscillation of antennal cAMP concentrations (Schendzielorz et al., 2015). This oscillation is driven by the circadian clock and serves as an input; the internal mechanism of the clock is not modeled explicitly. Arrows indicate the flow of ions through the channels. **(B)** Parametrized circadian oscillation in Orco conductivity, introduced as an external input to our model, representing the gating of Orco by cAMP whose concentration oscillates on a circadian timescale. The times of minimum and maximum cAMP concentration are indicated by colored arrows. **(C)** Parametrized IV curve of the Orco channel showing a linear behavior with the slope depending on the cAMP concentration. Line colors correspond to the arrows in **B. (D)** Markov-chain representing all possible states and transitions for each type of ion channel included in the model. The per capita transition rates (α and β) depend on membrane potential and in the case of the BK channel also on the intracellular Ca^{2+}-concentration. The "N" state vectors contain the population of channels in each state "n". Directed edges are numbered in red. The only conducting state of each ion channel, representing the condition where all its gates are open, is shown in green.

Results

We tested the hypothesis that sensory neurons, such as insect ORNs, perform active, anticipatory sensing based upon an endogenous plasma membrane clock with the pacemaker channel Orco as the core element. We focused on pheromone-sensitive long trichoid sensilla of male *M. sexta* hawkmoth antennae which express daily rhythms in pheromone sensitivity and temporal resolution that are controlled by a circadian clock. We performed minimally invasive *in vivo* tip recordings over the course of several days to search for daily rhythms in spontaneous spiking activity as a measure of endogenous membrane potential oscillations.

Pheromone-sensitive hawkmoth ORNs exhibit Orco-dependent circadian rhythms in spontaneous spiking activity

The ORNs that innervate the pheromone-sensitive long trichoid sensilla on male *M. sexta* antennae display spontaneous spiking patterns of irregular bursts with interspersed single action potentials in short-term recordings (Dolzer et al., 2001). In the present study we documented the same pattern in long-term recordings over the course of 2-7 days. This enabled us to search for daily and circadian rhythmicity in spontaneous ORN spiking activity in the absence of pheromone stimulation.

RAIN analysis of the spontaneous spiking patterns revealed significant daily rhythms in 7 of 11 animals under long-day conditions (17:7 h LD) (Figure 3A). The maxima in spontaneous activity occurred mostly during the dark phase when nocturnal hawkmoths are active (Figure 3A (top), Bi light blue arrow), and minima occurred during the light phase when hawkmoths rest/sleep (Figure 3A (bottom), Bi dark blue arrow). High spiking activity in the dark phase had a mean maximum frequency of ~3 Hz (delta range: 0.5 – 4 Hz) (Figure 3Bii). In contrast, the minimum spiking frequencies during the hawkmoth's resting phase were below 0.5 Hz (Figure 3A (bottom)).

Since ORN firing patterns had a clear daily rhythm in LD both in individual animals (Figure 3Bi) and averaged across animals (Figure 3Bii, Biii), we examined whether these rhythms depended on cycling light cues or whether they persisted in constant darkness (DD), as expected for an endogenous, circadian clock-driven rhythm. In DD, the spontaneous ORN firing pattern remained rhythmic (RAIN: 8 of 12 animals), albeit with less robustness: The single peak of high spiking activity that was observed at the same ZT across several days in LD divided into multiple bouts of high spiking activity in the activity phase in 8 of 12 animals (Figure 3Ci). Also, in DD conditions, the high spiking activity phase shifted into the subjective day due to the individual endogenous circadian periods of about 23.5 +/-2.8 h (21.27 h in Figure 3Ci). Using pheromone exposure as additional zeitgeber also did not synchronize the animals (Figure 3 – Supplement). Thus, averaging the instantaneous spiking activity across all DD animals did not depict clear circadian rhythms (Figure 3Cii). Therefore, we phase-aligned the mean frequency of spontaneous activity (see Methods). After alignment, circadian rhythms were visible across DD animals (Figure 3Ciii), comparable to the daily rhythms in LD (cf. Figure 3 Biii and Ciii).

Next, we examined whether Orco, a leaky, non-specific cation channel, is the dominant depolarizing pacemaker current of ORNs that drives circadian rhythms in spontaneous spiking activity. Infusion of the Orco antagonist OLC15 into the sensillum lymph obliterated circadian rhythms and attenuated the spontaneous activity in several, but not all experiments (RAIN: 2 of 12 animals expressed circadian rhythms) (Figure 3Di). This attenuation resulted in a linear decrease in spiking activity over several days (Figure 3Dii, Diii). Even after phase-aligning the individual experiments, no circadian rhythm was present in the average across all OLC15-treated animals (Figure 3Diii).

Because OLC15 is not membrane-permeable on its own it was infused with low concentrations (0.05%) of DMSO through the recording electrode into the sensillum lymph and, therefore, effectiveness increased over time. Hence, we fit the spiking activity of each animal and in each condition with linear regression lines over the whole recording time to compare the slopes of the

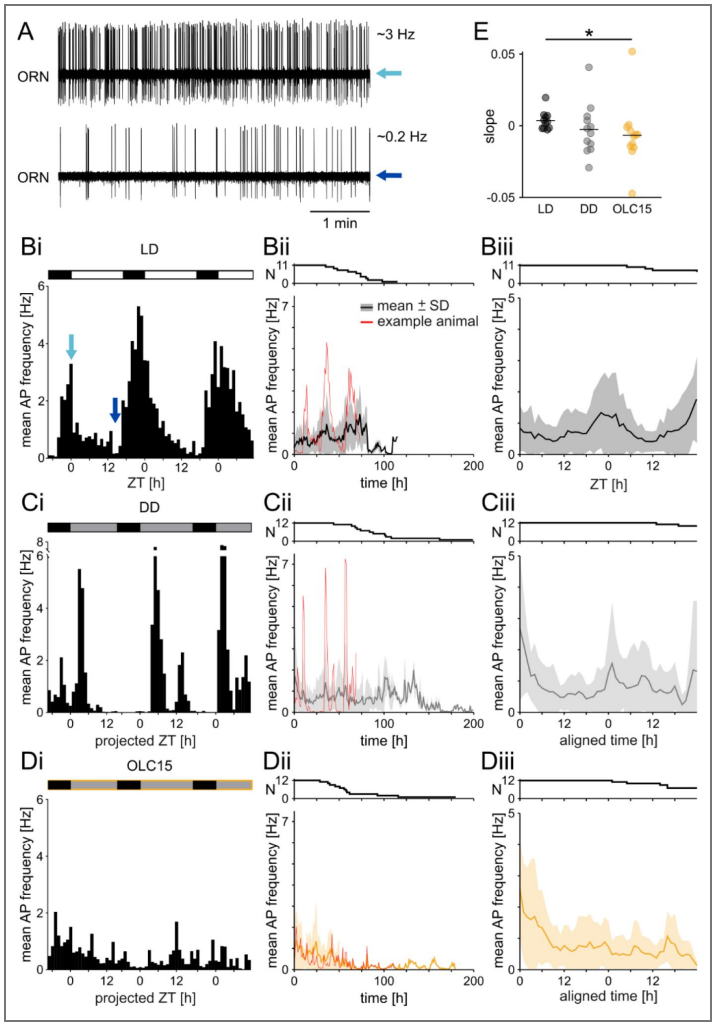

Figure 3. Spontaneous activity of pheromone-sensitive olfactory receptor neurons (ORNs) of male *M. sexta* shows Orco-dependent circadian modulation.

(A) Example tip recordings of the spontaneous activity of one long trichoid sensillum during a period of high (top, average frequency ~ 3 Hz) and low (bottom, average frequency ~ 0.2 Hz) activity. **(Bi)** Spontaneous spike frequency of one long-term ORN recording during 17:7 light-dark cycles (same experiment as in **A**, colored arrows indicate respective zeitgeber times (ZT)), indicated by the black-white bar at the top, increased during each activity phase and was low during the resting phases. Spike frequencies were averaged for each 1 h bin. **(Bii)** Mean spontaneous ORN spike frequency across all LD animals in 1 h bins. Data from the individual in **Bi** is highlighted in red. Recordings had different lengths, therefore the number of recordings used for the element-wise mean for each 1 h bin decreased with the time since the start of the recording, indicated in the top panel. **(Biii)** Mean spontaneous ORN spike frequency across all LD animals in 1 h bins during the first 48 hours revealed circadian activity. **(Ci)** The spontaneous spike frequency of one long-term ORN recording in constant darkness (DD, the expected times of lights on are represented by grey bars above) exhibited a circadian pattern. The peak activity shifted in DD due to the animal's endogenous, free-running circadian period τ = 21.27 h. **(Cii)** Mean spontaneous ORN spike frequency across all DD animals in 1 h bins. Data from the individual in Ci is highlighted in red. **(Ciii)** Mean spontaneous ORN spike frequency across all DD animals in 1 h bins during the first 48 hours after aligning the time to the first maximum in spontaneous activity (see Methods) revealed circadian activity. **(Di)** The spontaneous spike frequency of one long-term ORN recording in constant darkness with infusion of the Orco antagonist OLC15 (orange frame) dissipated the circadian rhythm of spontaneous activity. **(Dii)** Mean spontaneous ORN spike frequency across all OLC15 animals in 1 h bins. Data from the individual in **Di** is highlighted in red. In contrast to LD and DD conditions, the spike frequency decreases over time with prolonged exposure to OLC15. **(Diii)** Mean spontaneous ORN spike frequency across all OLC15 animals in 1 h bins (mean ± SD) during the first 48 hours after aligning the time to the first maximum in spontaneous activity (see Methods). In contrast to LD and DD conditions, the circadian change in spontaneous spiking frequency disappeared. **(E)** The slopes of the linear fits to the binned spiking activity of each individual animal in the three different conditions (see Methods). Each dot indicates the slope for one experiment. The line indicates the mean. The slope for OLC15 is significantly different from control LD.

fits (Figure 3E). In LD, the mean ± SD slope was 0.004 ± 0.006 Hz/h, indicating that the average spiking activity remained similar throughout the duration of the recording. In DD, the slope was -0.003 ± 0.018 Hz/h and was not different from LD. In contrast, the mean slope during OLC15 treatment was -0.007 ± 0.022 Hz/h, significantly smaller than in LD (ANOVA on ranks with Dunn's post-hoc test; H(2) = 7.681, p = 0.021). The negative slope corroborated the finding that spiking activity decreased over time in the presence of the Orco blocker.

Activity rhythms between hawkmoths desynchronize and have only weak phase coupling in the absence of pheromone stimulation, even in LD cycles (Ghosh et al., 2024). Therefore, we first determined the percentage of animals that expressed circadian rhythmicity (period of 24 ± 4 h) for each attribute with RAIN (Figure 4A). In LD, all attributes except #AP per burst and intra-burst frequency showed daily modulation in most animals. Circadian rhythms were still present in more than half of the animals in DD for mean spiking frequency, mean burst frequency, and mean event frequency. In contrast, the attributes of only a few animals remained rhythmic with the Orco channel blocker OLC15.

To further quantify the circadian differences, especially of the desynchronized animals, we compared different attributes of spontaneous activity between periods of high and low activity, for DD conditions after phase alignment (see Methods) instead of comparing fixed ZT or circadian time (CT) intervals. Despite the high variability in ORN spiking between individuals, the mean frequency of spontaneous ORN activity was significantly higher during the high activity phase than during low activity in both LD and DD recordings (Figure 4Bi, Bii). In LD, but not in DD, the frequency of bursting increased significantly during the high activity phase (Figure 4Ci, Cii). The percentage of spikes that are part of bursts was less variable and lower during the high activity phase in LD but not significantly different in DD (Figure 4Di, Dii). The mean burst duration was less variable during the high than the low activity phase in LD, but not significantly shorter in any condition (Figure 4Ei, Eii). Furthermore, both in LD and DD, the mean inter-event frequencies were significantly higher during the high activity phase (Figure 4Fi,Fii), indicating a significantly higher overall spontaneous spiking activity during the hawkmoth's activity phase. The mean number of spikes per burst, and intra-burst frequencies did not differ significantly between high or low activity periods in both LD and DD conditions (Figure 4Gi, Gii, Hi, Hii). The addition of Orco antagonist OLC15 deleted any significant differences of spontaneous activity found in LD and DD (Figure 4Biii-Hiii). In conclusion, the mean frequency of spontaneous spiking and the frequency of bursting expressed circadian modulation, and are both most likely controlled via a circadian clock that involves Orco.

Orco imposes circadian modulation on the ultradian rhythms in spontaneous ORN activity

After establishing that Orco influences the circadian changes in ORN spiking activity between the animal's resting and activity phase we examined if Orco also influences ORN spiking rhythms on the largely different ultradian timescales in the frequency range between 0.01-1000 Hz. In all conditions, two broad bands of ultradian instantaneous frequencies were evident: one upper band of >10 to ~100 Hz (beta/gamma range) and a lower band between 0.1 to ≤10 Hz (delta/theta/alpha range) (Figure 5). The upper band primarily represents the frequencies of spikes within a burst, while the lower band represents single spikes and frequencies between bursts.

In LD, two types of daily/circadian modulation of the ultradian frequencies occurred (Figure 5A). The upper frequency band was mostly modulated in prevalence (its frequency of occurrence) but not in its frequency range. The lower band was modulated both in prevalence and frequency range, which resulted in a sinusoidal change in the mean of the frequency band over 24 h. During the hawkmoth's activity phase, higher frequencies of up to ~10 Hz occurred, while frequencies dropped below 1 Hz during the resting phase. Because of this circadian increase in the lower frequency band, it merged with the high frequency band when both bands had maximum prevalence during the activity phase around ZT 0.

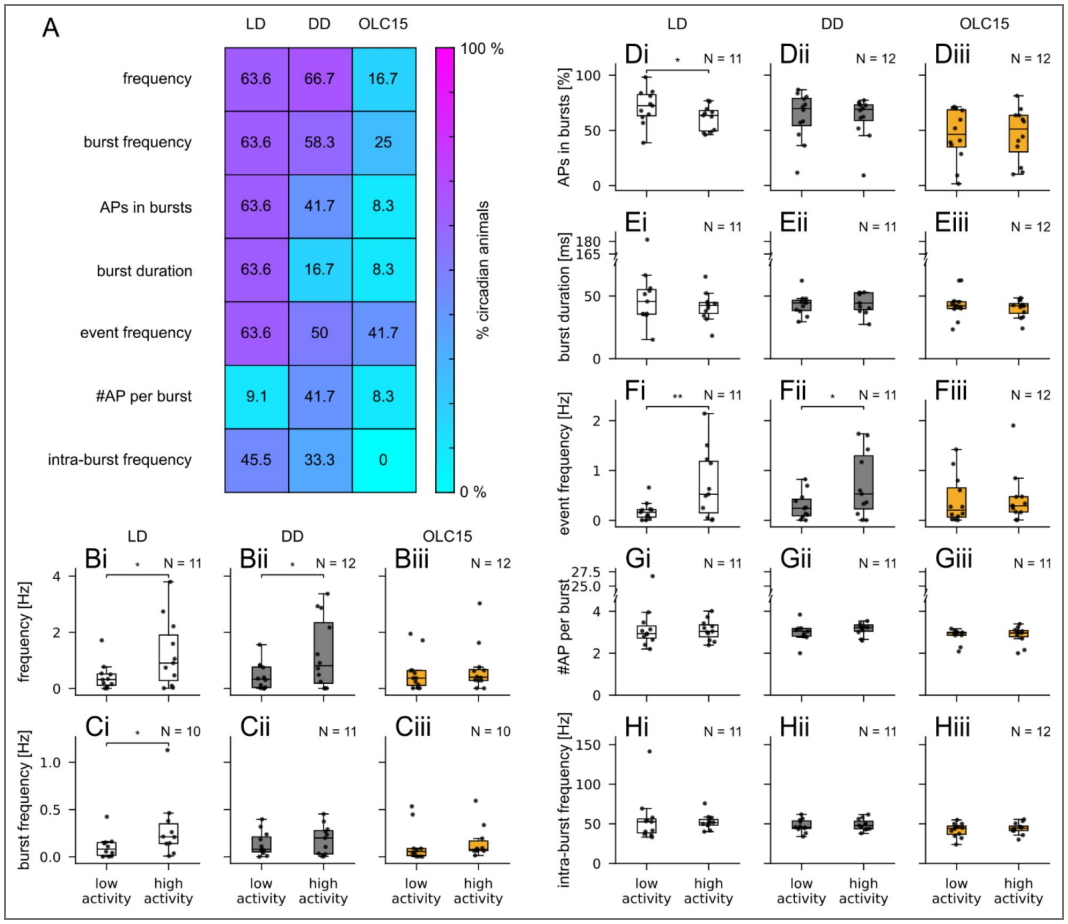

Figure 4. Blocking Orco removed circadian modulation of spontaneous ORN spiking patterns.

RAIN analyses demonstrated significant circadian rhythmicity for most animals in most attributes of the spontaneous spiking activity in LD and DD conditions but not in OLC15 (**A**). Values and background colors indicate the percentage of animals that expressed significant circadian rhythmicity. Circadian differences of attributes were further quantified between the time windows of low vs. high activity (Wilcoxon signed-rank test, α = 0.05; **B-H**). Significant differences occurred mostly in LD (white boxes) and DD (gray boxes) conditions, but never when Orco was blocked with OLC15 (orange boxes). In both LD and DD, the mean spiking frequency was increased during high activity (**Bi, Bii**). Only in LD but not in DD, the mean burst frequency (**Ci, Cii**) increased, whereas the relative number of spikes belonging to a burst (**Di, Dii**) decreased significantly during the high activity period. Both in LD and DD the mean event frequency (**Fi**,**Fii**) increased significantly. Mean burst duration (**Ei, Eii**), mean number of spikes per bust (**Gi**,**Gii**), and mean intra-burst intervals (**Hi, Hii**) did not differ between low vs. high spiking activity in LD and DD. When blocking Orco, the attributes for low vs. high activity did not differ for any of the attributes tested (**Biii-Hiii**). In DD and OLC15conditions, activity phases were aligned as described in the Methods; thus, low activity in DD was at subjective ZT 19 and in OLC15 at subjective ZT 13, high activity was in both cases at subjective ZT 24. ZTs for low and high activity in LD were 10 and 0, respectively.

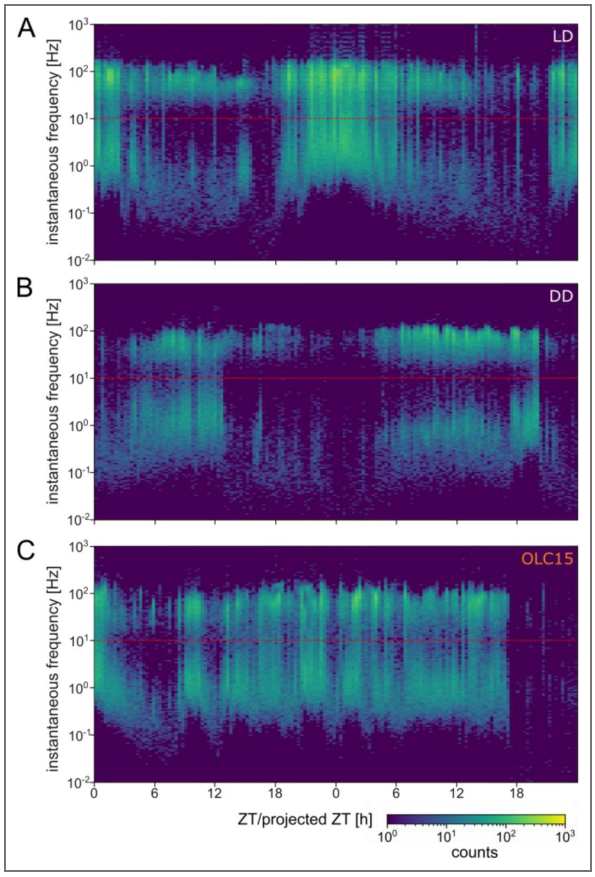

Figure 5. Blocking Orco removed circadian regulation of ultradian rhythms in the spontaneous ORN spiking pattern.

Heat map of the instantaneous frequencies (1/ISI) over two consecutive days of long-term tip recordings of one pheromone-sensitive long trichoid sensillum under different conditions (LD **(A)**, DD **(B)**, OLC15 **(C)**) in each panel. Representative recordings from one animal in each panel. Pixel color indicates the counts of instantaneous frequencies in that respective bin. The points fall mostly in a band of high frequencies (>10 – ~100 Hz) and low frequencies (0.01 – ~10 Hz), with the high-frequency band representing the instantaneous frequencies of spikes within a burst and the low-frequency band the instantaneous frequency between bursts. **(A, B)** The high frequency band indicates daily and circadian modulation of frequency prevalence. In addition, the low frequency band (<0.01 Hz to ~ 10 Hz) also displayed circadian modulation of the frequency composition. **(C)** Infusion of OLC15 deleted the circadian modulation in both frequency bands but not the ultradian rhythm of frequency prevalence.

The circadian modulation of both frequency bands was maintained in constant darkness (Figure 5B) but phase-shifted with respect to the projected ZT due to the endogenous circadian period of each individual. Again, this indicates that a clock is modulating the spontaneous ORN spiking activity over the course of a day. The addition of the Orco antagonist OLC15 deleted any circadian modulation of either frequency band. Interestingly, the instantaneous frequencies in both bands still showed correlated changes in prevalence and merging, but now at ultradian periods only.

Additional Fourier analysis (see Methods) of spontaneous spiking activity over the course of several days revealed faster ultradian and slower infradian rhythms, ranging from 0.6 h to 38 h, in addition to the circadian (24 ± 4 h) rhythm (Figure 6Ai, Bi, Ci). Some rhythms (factorials of 24 h, like 12 h, 6 h, etc.) appeared to be harmonics of the circadian rhythm, which were not excluded in our analysis. Most animals expressed ultradian rhythms of 2-4 h in LD as well as DD conditions. Fourier confirmed the decrease of animals with circadian spiking activity in OLC15 (58.3% in DD, 33.3% in OLC15). Please note that discrepancies in the number of animals with circadian rhythms between RAIN and Fourier/wavelet analyses are due to the fundamentally different sensitivities in methodology. In brief, Fourier analysis assumes a stationary sinusoidal component, whereas RAIN as a rank-based umbrella test detects consistent raise-fall patterns, including asymmetric rhythms. Nonetheless, both methods confirmed a dramatic decrease in animals with circadian spiking patterns in OLC15. In addition, 33.3% of animals expressed infradian spiking patterns (up from 0% in DD) with OLC15. Ultradian periods could be detected in all animals in all conditions but their distribution did not differ between conditions (1-way ANOVA;$F(2, 117) = 0.87$, $p = 0.421$). These results were corroborated by continuous wavelet analysis, which provided time-resolved spectral power across different rhythmic periods (Figure 6Aii, Bii, Cii).In control LD and DD conditions, wavelet power for ultradian periods increased during times of elevated firing rate and decreased during periods of low activity (Figure 6Aii and Bii, middle and bottom panels). This dynamic pattern indicates that ultradian rhythms were not constant over time but were instead modulated with a circadian rhythm, becoming more prominent during circadian peaks in neuronal activity. Such circadian gating of ultradian power was clearly visible in the wavelet spectrograms as alternating bands of higher and lower ultradian power aligned with daily activity cycles. Following Orco blockade with OLC15, this modulation was disrupted (Figure 6Cii middle panel): although ultradian components persisted (Figure 6Cii bottom panel), they no longer showed systematic variation with the circadian cycle, suggesting a decoupling of ultradian rhythms from circadian control.

Orco expression is not under the control of the molecular TTFL clockwork

So far, our results indicated a prominent role of Orco in the circadian modulation of ORN spiking activity. Since it is the general opinion that the master circadian clock is the TTFL clock that dominates all physiological and behavioral circadian rhythms via transcriptional control, we examined whether Orco transcript abundance shows a daily rhythm, as previously found for clock genes in hawkmoth antennae (Schneider et al., 2025; Schuckel et al., 2007). However, in contrast to the circadian clock gene *tim*, qPCR of whole male hawkmoth antennae across different ZTs revealed no significant daily rhythm of Orco transcript abundance (Figure 7; ANOVA on ranks, $H(5) = 6.91$, $p = 0.227$). Thus, we suggest that Orco function is controlled via a posttranslational circadian clockwork mechanism that is associated directly with the plasma membrane (Stengl and Schneider, 2024; Stengl and Schröder, 2021).

Circadian changes in Orco conductance are sufficient to modulate spiking activity in a computational model of a hawkmoth ORN

The maximum conductivity of *Drosophila* Orco as a leaky ion channel is modulated by cAMP (Getahun et al., 2013; Martín et al., 2001; Sargsyan et al., 2011; Wicher et al., 2008). In hawkmoth antennae, cAMP levels oscillate throughout the day and are involved in sensitizing the ORNs to pheromone (Dolzer et al., 2021; Flecke et al., 2010; Flecke and Stengl, 2009;

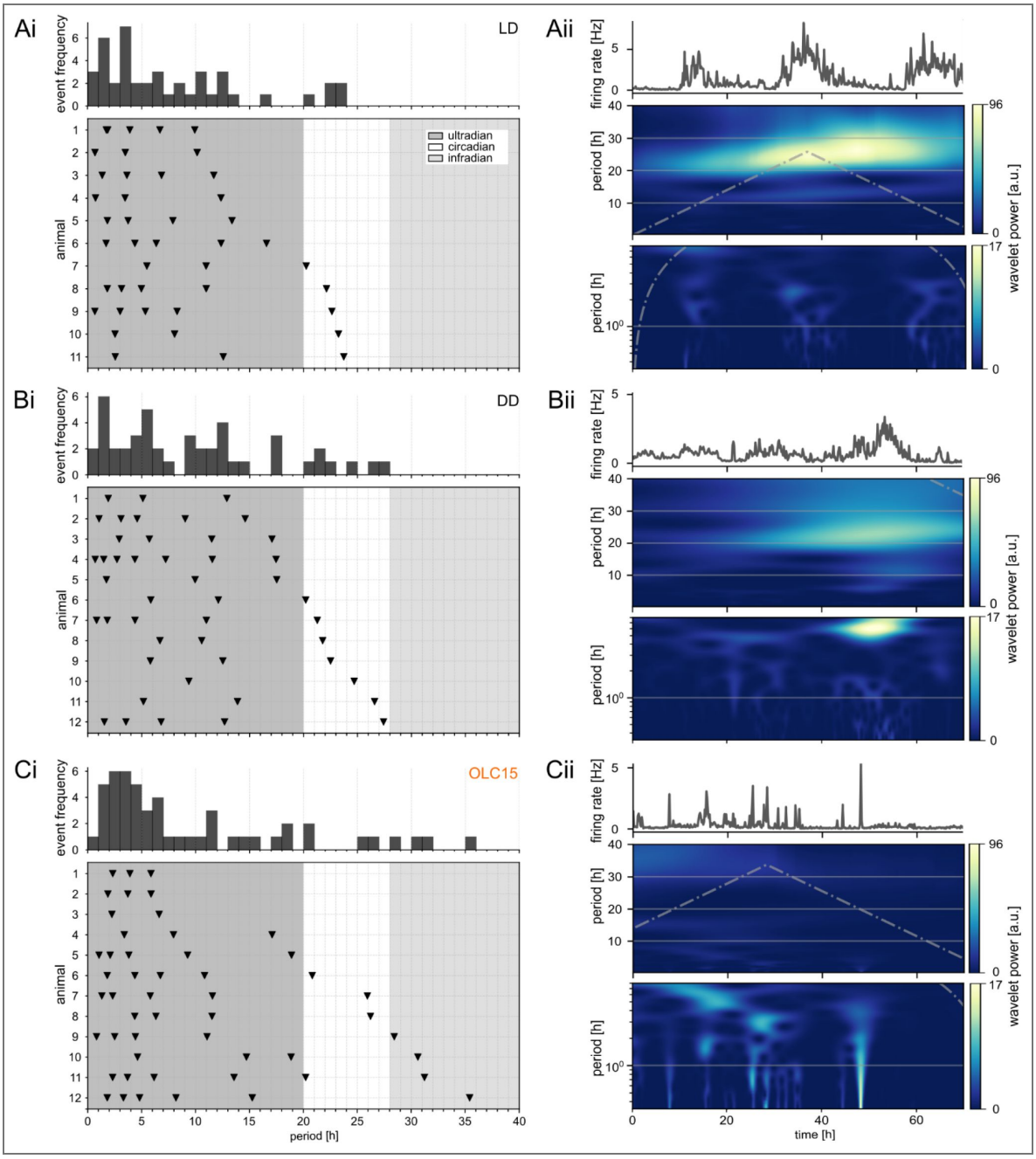

Figure 6. Blocking Orco affected ultradian and infradian frequencies in the spontaneous ORN firing patterns.

The Fourier analysis of spontaneous spiking activity revealed rhythms with ultradian (<20 h; dark grey), circadian (20-28 h; white), and infradian periods (>28 h; light grey) in LD (**Ai**), DD (**Bi**), and OLC15 (**Ci**). Each line represents one animal where each triangular marker is at the local maximum in the frequency spectra obtained for that animal. The histograms above illustrate how often specific periods of spiking activity rhythms occurred averaged over all animals. Circadian rhythms were detected in LD (N = 5 of 11), DD (N = 7 of 10), and OLC15 (N = 4 of 12). Wavelet analysis of LD (**Aii**), DD (**Bii**), and OLC15 (**Cii**) confirmed the occurrence of multiscale periods. Example plots for one animal each, the same animals as in Figure 5. For each panel, the top plot depicts the mean firing frequency, the middle plot the wavelet power in the same period range as panels **i**, and the bottom plot the wavelet power for infradian periods up to 7 h on a log scale to highlight infradian time scales. Gray dashed lines indicate cone of uncertainty.

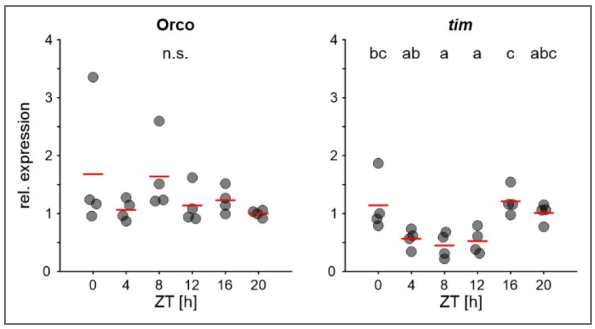

Figure 7. Orco is not under control of the TTFL-based molecular circadian clock.

Relative expression levels of *Orco* and *tim* mRNA from male hawkmoth antennae raised under LD conditions. *Orco* expression levels did not differ significantly between ZTs (ANOVA on ranks, H(5) = 6.91, p = 0.227: N = 4 per ZT). *tim* expression levels changed significantly throughout the day (1-way ANOVA, F(5, 18) = 6.215, p = 0.002) Red lines indicate mean, *tim* served as positive control.

Schendzielorz et al., 2014, 2015). Hence, cAMP modulation of Orco conductance could be a putative mechanism for the Orco-dependent circadian modulation of ORN spiking activity, integrating Orco in a circadian PTFL based membrane clockwork (Stengl and Schneider, 2024).

To test the hypothesis that Orco is a cAMP-dependent, leaky ion channel, we constructed an ORN model (Methods and Supplementary Material) and tuned the parameters to provide a quantitative match with the biological data. The developed model provides a unified description of experimental observations. For instance, the ORN model yields irregular spiking activity with a bimodal distribution, consisting of both bursts and isolated spikes, successfully reproducing the experimental recordings (Figure 8A). This suggests a unified mechanism underlying the initiation of both phenomena: If the pacemaker-driven depolarization reaches the Na^+ threshold a firing process begins, and at this point randomness determines if other slower ion channels responsible for bursting are sufficiently activated to sustain a burst of several spikes.

Additionally, the ORN model replicates the distribution of the number of spikes per burst, which follows a decreasing exponential trend in both experimental and simulated results (Figure 8B).The model also successfully reproduces the circadian modulation of spiking activity: the maximum firing rate occurs when the Orco conductance is maximal, whereas the maximum percentage of spikes that are part of bursts correlates with the lowest Orco conductance, resulting in antiphase oscillations, as were observed in the experimental recordings (Figure 8C).

The frequency prevalences in the model over several days clustered in two distinct frequency bands: an upper band that corresponds to the intra-burst frequencies and a lower band, corresponding to inter-burst frequencies (Figure 8D), in agreement with the biological experiments (Figure 5A, B). When circadian oscillations in Orco conductance were included, inter-burst frequencies showed significant circadian variations, whereas intra-burst frequencies remained relatively constant, reminiscent of the biological data. Notably, the simulation captured the experimentally observed “merging” effect, where the low frequency band approaches the top band during high-activity periods (Figure 8D).

This merging of spiking and bursting frequencies suggests that the system approached a bifurcation, transitioning from a bursting regime to tonic spiking activity. Further evidence for the near bifurcation condition of the neurons is the distribution of number of spikes per burst that followed a decreasing exponential trend in contrast to a constant value, or a bounded range of spikes per burst, which would be expected from a standard bursting neuron model (Figure 8B). The observation that the circadian modulation of spiking activity requires only one parameter, namely changes in the Orco conductivity, to describe the circadian effects on the ORN spiking pattern indicates the crucial role of the Orco channel in circadian control.

cAMP regulates the circadian function of Orco

Our computational model predicted that the daily/circadian oscillations in cAMP levels (Schendzielorz et al., 2015) control the circadian modulation of spontaneous spiking activity of hawkmoth ORNs. To test this prediction in hawkmoth ORNs, we increased cAMP levels by infusing 8-Br-cAMP-AM through the recording electrode into the sensillar lymph (Figure 9) at ZT 1-3. This significantly increased the mean frequency of the spontaneous spiking activity (Figure 9A; Wilcoxon signed-rank test $Z = -2.701$; $p = 0.004$). To check whether this increase in mean frequency was caused by direct or indirect interaction of cAMP with the Orco channel, we infused the Orco antagonist OLC15 together with 8-Br-cAMP-AM through the same recording electrode. Blocking Orco prevented a significant change in the spontaneous spiking frequency via the cAMP analogue (Figure 9B; paired t-test $t(9) = -1.446$; $p = 0.182$). This further corroborates cAMP-dependent modulation of the circadian pacemaker channel Orco.

Discussion

With *in vivo* long-term tip recordings of pheromone-sensitive long trichoid sensilla of male *M. sexta* hawkmoth antennae, we searched for a membrane-associated PTFL clockwork component that orchestrates membrane potential oscillations to facilitate active sensing of pheromone

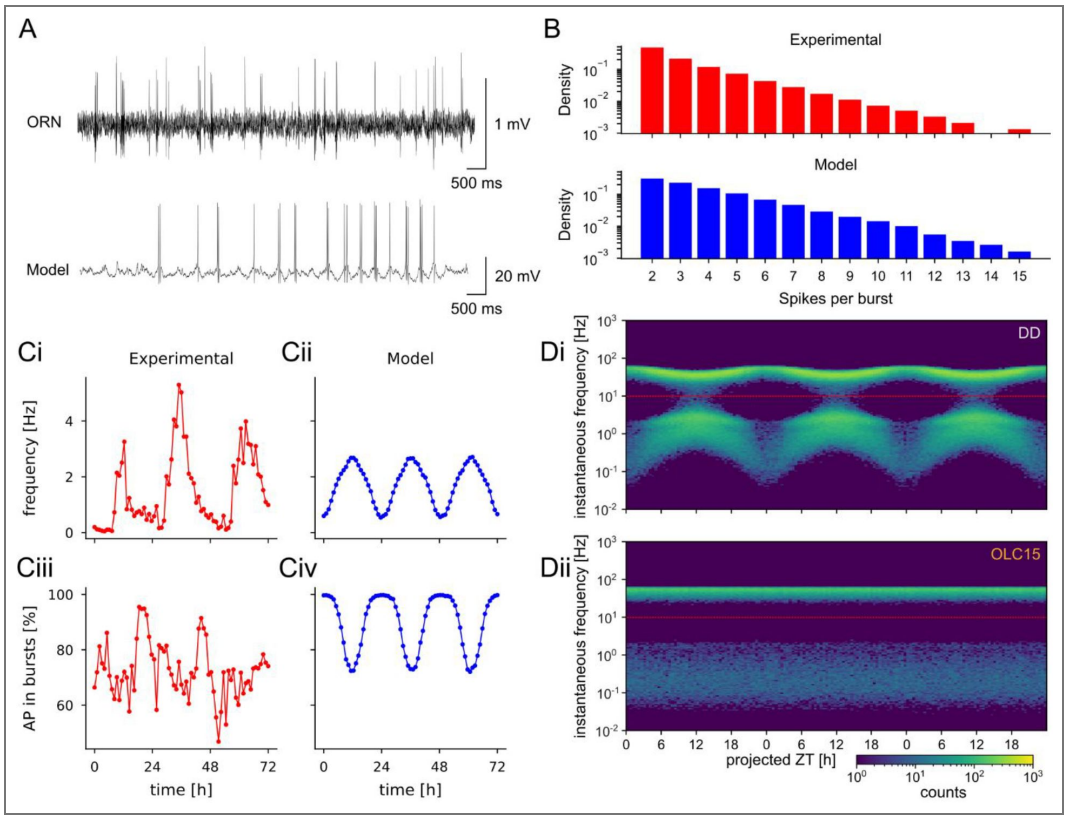

Figure 8. The model adequately reproduces the firing pattern of the biological ORN.

(A) The model activity (bottom trace) displays both isolated spikes and bursts of variable length as in the original recording (top trace). The model represents an intracellular recording whereas the biological recordings were done with extracellular electrodes. **(B)** Semi-logarithmic plot of burst length distribution of an experimental LD recording (top) and simulated model (bottom) of spontaneous action potential activity of pheromone-sensitive neurons. Both the model and the recordings display exponential decrease of the count's density as a function of the burst length, shown as a linear decrease in the logarithmic scale. **(C)** Comparison of the circadian modulationof model and ORN spiking attributes. Top panels (**Ci, Cii**) show mean spike frequency, whereas bottom panels (**Ciii, Civ**) show the percentage of spikes belonging to bursts. The simulated model reproduced the circadian dynamics observed in the experimental recordings, demonstrating good agreement between model and biological data. **(D)** Heat map of the simulated model, pixel color indicates the density of instantaneous frequencies in that respective bin. The points can be roughly divided in a band of high frequencies (top, ~50 – 80 Hz) and low frequencies (bottom, ~0.1 – 5 Hz), with the high-frequency band representing the instantaneous frequencies of spikes within a burst and the low-frequency band the instantaneous frequency between bursts. **(Di)** Simulated spikes with circadian regulation by the Orco channel; the inter-burst frequencies varied widely with circadian rhythmicity while the frequencies within burst remained approximately constant. The simulated results also reproduced the "merging" effect between the two bands when the bottom one approaches the top one. **(Dii)** Simulated spikes without circadian regulation of Orco had no circadian oscillations.

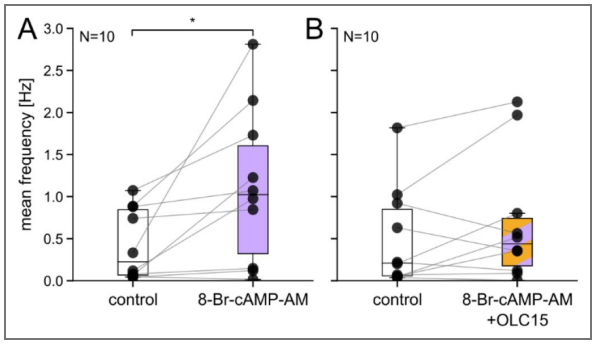

Figure 9. **cAMP modulates open-time probability of Orco in *M. sexta*.**

Perfusion of 8-Br-cAMP-AM significantly increased the spontaneous spiking activity at the end of the activity phase (ZT 1-3; **A**; Wilcoxon signed-rank test Z = -2.701; p = 0.004). However, activity did not increase when 8-Br-cAMP-AM was added together with the Orco blocker OLC15 (**B**; paired t-test t(9) = -1.446; p = 0.182). Electrodes were filled with SLR containing 0.1% and 0.15% DMSO as control in **A** and **B**, respectively. Data from individual animals are connected by lines.

patterns during mating flights. Indeed, we detected interlinked circadian and ultradian frequencies in the spontaneous spiking activity, indicative of underlying membrane potential oscillations in ORNs. We found that the olfactory receptor co-receptor (Orco) acts as a pacemaker channel that controls the circadian modulation of the spiking activity without affecting the ultradian frequency ranges that are relevant for the primary fast, phasic pheromone response (Dolzer et al., 2003; Nolte et al., 2016; Schneider et al., 2025). Our computational model confirmed that the circadian modulation of open-time probability of Orco as a leaky pacemaker channel was sufficient to account for our experimental results. Since Orco was not under circadian transcriptional control of the TTFL present in hawkmoth ORNs, our findings are consistent with our novel hypothesis that the ORN's plasma membrane constitutes an endogenous, plastic post-translational feedback loop (PTFL) clockwork. Consistent with experimental data (Schendzielorz et al., 2015), we propose that PTFL-generated endogenous multiscale membrane potential oscillations comprising interlinked oscillations in Ca^{2+} and cAMP levels provide circadian modulation of Orco conductance rather than TTFL-commanded circadian Orco transcription and turnover.

The expression of a 2^{nd} messenger-dependent pacemaker/leak channel in ORNs that does not require daily transcription would constitute an economic and rapidly adjustable mechanism of active sensing. It could generate endogenous membrane potential oscillations that are tuned to detect and resonate with behaviorally relevant temporal patterns of zeitgeber signals, such as the circadian and ultradian pheromone fluctuations in the insect's environment (Stengl and Schneider, 2024; Stengl and Schröder, 2021). The present study provides the first evidence for a systems view of biological timing that involves a PTFL membrane clock in insect sensory neurons, instead of the prevailing hierarchical view that assumes all endogenous circadian oscillations are outputs of the genetic TTFL clock (Stengl and Schneider, 2024; Stengl and Schröder, 2021).

Orco acts as a pacemaker channel that controls membrane potential oscillations underlying spontaneous ORN spiking activity

The resting membrane potential of most silent neurons lies close to the negative equilibrium potential for potassium ions, mainly due to potassium leak channels (Goldstein et al., 2001; Hille, 2001; Patel and Honoré, 2001; Talley et al., 2001). Spontaneously active neurons require the expression of leak or pacemaker channels that open at the hyperpolarized resting membrane potential, thus depolarizing the neuron(Bose et al., 2014; Cochet-Bissuel et al., 2014; Das et al., 2016; Golowasch et al., 2017; Lüthi and McCormick, 1998; Ratliff et al., 2021; Robinson and Siegelbaum, 2003; Sharma et al., 2023). When the pacemaker-driven depolarization reaches spike thresholds, voltage-gated Na^+, K^+ and Ca^{2+} channels promote Ca^{2+} influx and spiking. Voltage- and Ca^{2+}-gated hyperpolarizing K^+ channels then repolarize the neuron to negative membrane potentials, re-starting the cycle. Thus, membrane potential oscillations with interlinked oscillations in intracellular Ca^{2+} levels drive spontaneous spiking activity which depends on the type of pacemaker channel and antagonistic ion channels present.

In insect ORNs, at least two types of pacemaker channels exist: the highly conserved, slow, leaky Orco, which we focus on in this study, and an inversely voltage-dependent HCN type channel (Butterwick et al., 2018; Dolzer et al., 2021; Kodirov, 2022; Lee and MacKinnon, 2017; Mandala et al., 2025; Nolte et al., 2016, 2013; Sato et al., 2008; Stengl and Funk, 2013; Stengl and Schneider, 2024; Stengl and Schröder, 2021; Wicher et al., 2008; Wicher and Miazzi, 2021). When expressed *in vitro* in heterologous expression systems, *Drosophila* as well as *Manduca* Orco homo- and heteromers assemble into leaky, non-specific cation channels with a reversal potential around 0 mV, constitutively leaking Na^+, K^+, and Ca^{2+} into ORNs (Nolte et al., 2016, 2013; Sato et al., 2008; Stengl and Funk, 2013; Wicher et al., 2008; Wicher and Miazzi, 2021). Thus, while this study did not aim to unravel the overall generation of spontaneous activity in ORNs, here, we examined whether the leak channel Orco in hawkmoth ORNs is the core pacemaker channel responsible for membrane potential oscillations that drive spontaneous circadian activity (Stengl, 2010; Stengl and Schneider, 2024).

Differential location and function of Orco homo-or heteromers in the distinct membrane compartments of ORNs that face different ionic environments appear likely (Stengl and Funk, 2013; Stengl and Schröder, 2021). We propose that homomeric *Manduca* Orco pacemaker channels, as core element of a PTFL membrane clock, are restricted to the soma/inner dendrite compartment of ORNs (Stengl and Schneider, 2024; Stengl and Schröder, 2021). In contrast, we expect *Manduca* Orco heteromers to serve as obligatory chaperons to maintain ORs in the ciliary membranes, as proven in *Drosophila* (Benton et al., 2006). Since the ciliary compartment faces very high concentrations of K^+ in the sensillum lymph, matching intracellular K^+ levels (Kaissling and Thorson, 1980; Steinbrecht, 1992), we propose that Orco in ciliary membranes remains closed via unknown mechanisms, while Ca^{2+} channels of the TRP ion channel family serve the primary events of pheromone transduction (Gawalek and Stengl, 2018; Stengl, 1994, 1993). Otherwise, Orco channel opening would clamp the ciliary membranes at 0 mV, strongly reducing the driving force of pheromone-dependent receptor currents, not allowing for the ORN's extreme pheromone sensitivity (Stengl and Funk, 2013).

In support of this hypothesis, in both *Drosophila* (Benton et al., 2006) and *Manduca* (Nolte et al., 2016), Orco antisera labeled Orco in two of the three sealed off ORN membrane compartments: in the membranes of soma/ inner dendrite compartment, as well as in the membrane of outer cilia, but not in the axons of ORNs. In contrast, antisera against an OR in *Drosophila* detected ORs only in ciliary membranes but not in the other compartments of ORNs. Thus, the colocalization of OR-Orco heteromers only in cilia confirm that Orco is an obligatory coreceptor and chaperone of ORs localizing and maintaining the OR-Orco complexes in the ciliary membrane (Benton et al., 2006). Since antisera against *Manduca* ORs are not available, we do not known whether the pheromone-sensitive OR-Orco heteromers are solely located to ciliary membranes also in the hawkmoth while Orco homomers are found in the soma/inner dendrite compartment (Fandino et al., 2019). However, we know that Orco exists as homomeric complexes in wild-type hawkmoth ORNs because Orco expression starts during development well before ORs are present and because Orco agonist VUAA1 activates Orco in primary cell cultures of not yet pheromone-sensitive maturing ORNs (Nolte et al., 2016; Schweitzer et al., 1976).

In summary, we propose Orco to be a 2^{nd} messenger cascade-dependent core element of a PTFL membrane clock that is located in the soma/inner dendrite compartment of ORNs, which controls the ORN's membrane potential and is coupled to - but not dominated by - the TTFL clock in the hawkmoth ORNs (Schuckel et al., 2007; Stengl and Schneider, 2024).

Orco is suggested to be a second messenger-dependent control hub of a PTFL membrane clock that regulates circadian membrane potential oscillations in hawkmoth ORNs

Different 2^{nd} messenger cascades regulate *Drosophila* Orco via Ca^{2+}/calmodulin and via phosphorylation/de-phosphorylation at multiple sites (Cao et al., 2016; Getahun et al., 2016; Guo and Smith, 2017; Mukunda et al., 2016, 2014; Sargsyan et al., 2011). The Ca^{2+}/calmodulin binding site controls the localization of the OR-Orco complex in the ciliary membrane of ORNs, provides for negative feedback control of Orco conductance, and depends on previous odor stimulation (Bahk and Jones, 2016; Cao et al., 2016; Guo and Smith, 2022; Jain et al., 2021). After phosphorylation of Orco by protein kinase C (PKC), Orco directly or indirectly becomes cyclic nucleotide-dependent, with cGMP and cAMP increasing its open-time probability (Getahun et al., 2013; Wicher et al., 2008). While we do not know the second messenger-dependent modulation of hawkmoth Orco, due to Orco's highly conserved structure we assume similar Ca^{2+}/calmodulin-, PKC-, and cyclic nucleotide-dependent control of Orco's localization and open-time probability.

Since blocking Orco in *M. sexta* decreased the spontaneous activity and deleted its circadian but not ultradian modulation, Orco is apparently the main target for modulation of circadian activity in hawkmoth ORNs. The ultradian rhythms in spontaneous activity are presumably controlled by additional pacemaker channels. Since Orco transcript abundance was constant throughout the

day, Orco is not controlled directly by the circadian TTFL clock. Rather, a self-assembling PTFL membrane clock controls open-time probability and/or membrane localization of Orco via posttranslational modifications in a circadian manner. Because circadian rhythms in cAMP levels and phase-leading circadian rhythms in IP_3 were found in hawkmoth antennae (Schendzielorz et al., 2015), it is likely that Orco's phosphorylation state regulates its cAMP dependence in a daily rhythm. Indeed, our results showed that the increase of spontaneous activity caused by 8-Br-cAMP application is canceled with co-application of the Orco blocker OLC15. Thus, we assume that a PTFL membrane clock determines the circadian oscillations in the pheromone sensitivity and temporal resolution of ORNs via Ca^{2+}, PKC, and cAMP-dependent membrane potential control (Dolzer et al., 2021, 2008; Flecke et al., 2010, 2006; Redkozubov, 2000; Schendzielorz et al., 2015, 2012; Ziegelberger et al., 1990).

Our hypothesis that a circadian PTFL membrane clock in hawkmoth ORNs controls circadian rhythms in spontaneous spiking activity predicts that this PTFL clock comprises a membrane signalosome with the pacemaker channel Orco as central control hub (Stengl and Schneider, 2024). In the soma/inner dendrite compartment of the ORNs the protein complexes of this PTFL signalosome would generate the specific ultradian and circadian frequencies of endogenous potential oscillations, linked to oscillations of Ca^{2+} and cAMP that determine physiological setpoints of the ORN during circadian sleep-wake cycles. Thus, the PTFL membrane clock that generates endogenous membrane potential and Ca^{2+} level oscillations minimally consists of depolarizing, Ca^{2+} permeable Orco, voltage-gated Ca^{2+}, and hyperpolarizing K^+ channels. In the same PTFL soma clock, membrane-anchored adenylyl cyclases (ACs) and phosphodiesterases (PDE), that are antagonistically controlled by intracellular Ca^{2+} levels, are proposed to generate circadian cAMP oscillations (Halls and Cooper, 2011). Kinases, such as PKC and PKA, could couple potential oscillations with cAMP oscillations that target Orco, phosphatases, and PDEs via negative feedback. Very likely, this membrane PTFL clock is interlinked with metabolic clocks such as PTFL clocks that generate endogenous rhythms of redox elements or ATP availability (Edgar et al., 2012), as evident in, e.g., human red blood cells, which lack a nucleus (O'Neill and Reddy, 2011).

Furthermore, this PTFL-clock could contain octopamine receptors that couple to endogenous oscillations of intracellular Ca^{2+} and cAMP levels through activation of $G_{\alpha o}$ and $G_{\alpha s}$, as found in hawkmoths (Dacks et al., 2006; Flecke et al., 2010). Since octopamine levels in the hemolymph exhibit circadian oscillations and octopamine sets a physiological state of heightened alertness in insects, the circadian PTFL clock in ORNs would synchronize with endogenous physiological rhythms via octopamine receptor activation (Flecke and Stengl, 2009; Schendzielorz et al., 2015). This also constitutes a possible pathway to synchronize the ORN PTFL clock with circadian TTFL clocks in both ORNs and the brain. In horseshoe crab, the master clock sends multiscale patterned spike trains through retinal efferents at night, which carries information about the circadian phase and enhances visual sensitivity based on octopamine release and Camp signaling (Battelle, 2013; Liu and Passaglia, 2011). In *M. sexta*, two biogenic amine-immunoreactive neurons project into the sensory cell layer of the antenna, being suited to phase-shift endogenous cAMP oscillations via stress signals such as octopamine (Flecke and Stengl, 2009; Schendzielorz et al., 2015). Comparably, the circadian pacemaker center controls endogenous rhythms in the electrical network activity in rodent brains via endogenous cAMP oscillations that are phase-controlled through G-protein coupled receptor signaling (Ono et al., 2023; Prosser et al., 1989; Prosser and Gillette, 1991). Future studies will explore the links between PTFL and TTFL clocks in ORNs.

Circadian and ultradian rhythms in spontaneous ORN activity resemble the physiologically relevant timescales for active sensing

Moths are more sensitive to pheromone stimulation during their activity phase than at rest, apparently due to antennal circadian clocks (Flecke et al., 2010; Flecke and Stengl, 2009; Merlin et al., 2007, 2006; Schendzielorz et al., 2015; Schuckel et al., 2007; Silvegren et al., 2005). The greater the distance from the female, the lower the frequency of pheromone

filaments in the air. The increased pheromone sensitivity during the activity phase enhances the male's chance to detect and locate a calling female. Pheromone concentration is encoded in the frequency of the first, phasic burst of spikes of the characteristic triphasic spiking sequence of ORNs in response to brief pheromone pulses, which is independent of Orco (Dolzer et al., 2003; Nolte et al., 2013; Schneider et al., 2025). Consistent with these results, we found here that blocking Orco does not affect the upper frequency band of spontaneous activity that correlates with the frequency ranges of the pheromone-encoding primary fast pheromone response(Dolzer et al., 2003; Nolte et al., 2016, 2013). However, through the cAMP-dependent increase in Orco conductance during the activity phase, the ORN membrane potential is closer to spike threshold and fewer pheromone molecules are necessary to produce a receptor current that brings the membrane voltage over that threshold. Thus, larger Orco conductance increases the likelihood of an ORN response to pheromone stimulation without changing the typical triphasic spiking pattern of the response.

In the odor transduction of *Drosophila*, OR-Orco activation drives the initial receptor current response (Sato et al., 2008; Wicher et al., 2008). In contrast, Orco is not part of an OR-Orco odor-gated receptor ion channel complex in hawkmoths but controls the spontaneous ORN activity and the late, long-lasting pheromone response (LLPR). The LLPR begins several hundred milliseconds after the initiation of the pheromone-dependent transduction current and correlates with the time course of pheromone-induced rises in cGMP levels, possibly playing a role in odor memory or long-term gain control (Boekhoff et al., 1993; Nolte et al., 2016, 2013; Stengl, 2010; Stengl et al., 2001; Wicher and Miazzi, 2021; Ziegelberger et al., 1990). Thus, in hawkmoths, Orco is not part of the primary transduction channel but rather controls membrane potential oscillations and thereby the temporal resolution and general pheromone sensitivity of ORNs. In addition, the increased spontaneous burst frequency during the hawkmoth's activity phase improves the resolution of the anticipated pheromone pulses during its mating flight in search for females.

In the mammalian suprachiasmatic nucleus (SCN), the clock that controls the sleep-wake cycle, cAMP levels oscillate at an circadian frequency, and cAMP and cGMP induce ZT-dependent opposing phase shifts in SCN spiking activity (Prosser et al., 1989; Prosser and Gillette, 1991). In antennae of both *M. sexta* (Schendzielorz et al., 2015) and the cockroach *Rhyparobia maderae* (Schendzielorz et al., 2012), cAMP levels express daily and circadian oscillations and peak during the activity phase. In contrast, cGMP levels do not oscillate under constant conditions. They are in antiphase to the daily oscillations in cAMP levels in LD and are elevated by strong or long pheromone exposure, which adapts the sensitivity and temporal resolution of ORNs (Boekhoff et al., 1993; Dolzer et al., 2021; Flecke et al., 2006; Schendzielorz et al., 2015; Ziegelberger et al., 1990). This implies that cAMP and cGMP may have ZT-dependent effects on Orco conductivity, thereby affecting pheromone sensitivity via control of the membrane potential and intracellular Ca^{2+} concentrations.

The upregulation of neural activity during wakefulness/alertness seems to be ubiquitous among different species. For example, the many synchronously recorded neurons in human EEG show fast oscillations in the alpha, beta, and gamma frequency ranges during alertness and slow oscillations in the delta and theta ranges during rest and sleep. Similarly, in the lower frequency band, the spontaneous spiking activity of hawkmoth ORNs changes from below delta during rest to theta/alpha ranges during their activity phase. The upper frequency band in the gamma range, which did not depend on Orco regulation, comprises the spike frequency within a burst, reminiscent of the first phasic pheromone response that encodes pheromone concentration changes (Dolzer et al., 2003). The increased spontaneous spiking activity in the theta/alpha range during the activity phase of the hawkmoth matches the maximal temporal resolution of pheromone pulses of up to 10 Hz (Marion-Poll and Tobin, 1992), which supports a role for Orco as part of a membrane-bound PTFL clockwork that tunes the ORNs for active sensing. Even through oscillations in the field potential of electroantennogram responses to odor stimulation can reach 100 Hz in different insects (Szyszka et al., 2014), these frequencies most likely do not encode the temporal resolution of physiological odor responses. Apparently, they reflect the

astounding adaptive ability of antennal ORNs to synchronize their endogenous membrane potential oscillations across the antenna to a broad range of stimulation frequencies. Pheromone pulse resolution of about 100 Hz was never reported in single olfactory sensilla recordings, and in behavioral experiments male moths stopped their upwind mate search if pheromone pulses exceeded 30 Hz, apparently due to adaptation (Baker et al., 1985; Bau et al., 2005, 2002; Tripathy et al., 2010).

Circadian oscillations in the ORN membrane potential would be ideally suited to tune sensitivity and temporal resolution of the pheromone-sensitive ORNs to the hawkmoth's rest-activity cycle, synchronizing male and female mating behavior. Here, we have demonstrated how modulation of a leaky pacemaker channel can achieve these circadian oscillations. Whether cAMP levels are under control of the TTFL clock or oscillate based on Ca^{2+} concentration oscillations, and would therefore be part of a stand-alone PTFL clock, remains to be studied.

Stochastic ion channel dynamics and circadian modulation of Orco conductance explain modeled ORN firing patterns

Our modeling results provide mechanistic insight into the irregular spontaneous activity of pheromone-sensitive ORNs in *M. sexta*, highlighting how stochastic ion channel dynamics and circadian modulation of ion conductance together shape spiking patterns. By employing a Langevin approximation of the stochastic HH formalism, we demonstrate that the intrinsic noise arising from the random gating of ion channels is sufficient to generate both isolated spikes and bursts of spikes, as observed experimentally. Our model effectively recapitulates the spike distributions found *in vivo* and accounts for the role of channel noise as a critical determinant of ORN firing patterns.

A key contribution of our model is the incorporation of the Orco ion channel as a pacemaker component, with a conductance that varies linearly with cAMP concentration. We show that circadian modulation of Orco conductance alone is sufficient to produce the observed time-of-day dependent changes in spike distribution. This finding suggests that the rhythmic expression of cAMP levels across the circadian cycle may act as a primary driver of diurnal changes in ORN excitability, without requiring additional external inputs or modulation of other ion channels.

Importantly, our results reveal that the same set of ion channels can support the emergence of both single action potentials and complex bursting behaviors purely through the stochastic variability of their gating kinetics. This unifying explanation reduces the need for invoking separate biophysical mechanisms or circuit-level inputs to explain these distinct firing modes.

For simplicity, the circadian variation in cAMP concentration was modeled using a sinusoidal function. While this approximation is sufficient for capturing the qualitative features of the rhythmic modulation, future work could enhance the biological realism of the model by coupling Orco conductance dynamics to a molecular circadian oscillator, such as a Goodwin-type TTFL.

Incorporating this layer would allow for a more detailed exploration of how molecular clock components regulate cAMP synthesis and degradation. Additionally, further extensions could include downstream regulatory mechanisms such as phosphorylation and dephosphorylation events mediated by kinases and phosphatases under circadian control, potentially contributing to fine-tuned modulation of ion channel function over the daily cycle.

Together, these findings demonstrate the value of a biophysically grounded, noise-inclusive modeling framework for understanding complex temporal patterns in sensory neuron activity and open the door for future integrative models linking molecular circadian clocks to cellular excitability.

Supplementary Material

Mathematical Model

The mathematical model is a 22-dimensional system of stochastic differential equations designed to describe the behavior of ion channels and their effects on the membrane potential. I_{LVA} represents a low-voltage-activated calcium current, while I_{Na} and I_{K} are the transient sodium and potassium currents responsible for action potential generation. I_{BK} is a large-conductance potassium channel that is activated by both a depolarized membrane potential and an increased intracellular calcium concentration, and I_{L} is the leak current. Additionally, the Orco channel is a leaky, non-specific ion channel gated by cAMP, with the cAMP concentration oscillating in a circadian rhythm. To model the Orco conductance, we used a sinusoidal function of Zeitgeber time (ZT), independent of the membrane potential, as shown in Figure 2B, C. Each of these ion channels has been reported in vitro in previous studies (Dolzer et al., 2021).

The deterministic part of the 22D model is given by the mean field of the channel-based Langevin model. This approach was introduced by Fox and Lu's (1994) for a 14D HH model. In their framework, one dimension tracks the membrane potential, while the other 13 dimensions correspond to the fraction of channels in each of the five states in the potassium (K^+) Markov chain and the eight states in the sodium (Na^+) Markov chain. Pu and Thomas (2020) demonstrated that the deterministic 14D model and the original 4D HH model are dynamically equivalent, meaning that each solution of the 4D model corresponds to a solution of the 14D model.

Expanding upon Pu and Tomas' methodology to represent out system, we added one dimension to track the calcium concentration, six dimensions for each possible state of the LVA channel, and two dimensions for each possible state of the BK channel. The state vectors for each ion channel are therefore defined as follows: a five-component vector NK for the K^+ gates, an eight-component vector NNa for the Na^+ gates, a six-component vector NLVA for the LVA gates, and a two-component vector NBK for the BK gates. The state vectors are represented as:

$$N^K = [n_{K0}, n_{K1}, n_{K2}, n_{K3}, n_{K4}]^T \in [0,1]^5 \tag{1}$$

$$N^{Na} = [n_{Na00}, n_{Na10}, n_{Na20}, n_{Na30}, n_{Na01}, n_{Na11}, n_{Na21}, n_{Na31}]^T \in [0,1]^8 \tag{2}$$

$$N^{LVA} = [n_{LVA00}, n_{LVA10}, n_{LVA20}, n_{LVA01}, n_{LVA11}, n_{LVA21}]^T \in [0,1]^6 \tag{3}$$

$$N^{BK} = [n_{BK0}, n_{BK1}]^T \in [0,1]^2 \tag{4}$$

The K^+ channel consists of four independent n (activation) gates, forming a five-vertex channel-state diagram with eight directed edges. The channel conducts a current only when it is in the rightmost state (Figure 2D). Similarly, the Na^+ channel is composed of three identical n gates and one h (inactivation) gate, forming an 8-vertex diagram with 20 directed edges, one of which is conducting. The LVA channel includes two identical n gates and one h gate, resulting in a 6-vertex diagram with 14 directed edges, one of which is conducting. The BK channel consists of a single n gate, forming a 2-vertex diagram with two directed edges, one of which is conducting. The Markov chain for every channel is shown in Figure 2B.

For a sufficiently large number of channels, Schmidt and Thomas (2014) and Schmidt et al. (2018) demonstrated that, under voltage clamp, the equations governing the system can be approximated by a multidimensional Ornstein-Uhlenbeck (OU) process, or Langevin equation, as follows:

$$dN^{ion} = \sum_{k=1}^{k_{\max}} \zeta^{ion} \left\{ \alpha_k^{ion}(V) N_{i(k)}^{ion} dt + \sqrt{\epsilon^{ion} \alpha_k^{ion} N_{i(k)}^{ion}} dW_k^{ion} \right\} \quad (5)$$

Here $\zeta^{ion}$is the stoichiometry vector for the kth directed edge. If we write i(k) for the source node and j(k) for the destination node of edge k, then $\zeta^{ion} = e_{j(k)}^{ion} - e_{i(k)}^{ion}$. The voltage-dependent per capita transition rate along the kth edge is $\alpha_k^{ion}(V)$ and $N_{i(k)}^{ion}$ is the fractional occupancy of the source node for the kth transition. The finite-time increment in the Poisson process is approximated by a gaussian process, namely, the increment dW_k^{ion} in a Wiener (Brownian motion) process associated with each directed edge. These independent noise terms are scaled by $\epsilon^{ion} = \frac{1}{N_{\text{Tot}}^{ion}}$, where $\frac{1}{N_{\text{Tot}}^{\text{ion}}}$ represents the total number of that specific ion channel.

The membrane potential is governed by the current balance equation:

$$C \frac{dV}{dt} = \sum_{\chi} I_{\chi} \quad (6)$$

where the set χ contains the six ionic currents included in the model:

$$\chi \in \{LVA, Na, K, BK, L, ORCO\} \quad (7)$$

Each of the six ionic currents included in the model are described as:

$$I_{Na} = -g_{Na} N_8^{Na} (V - V_{Na}) \quad (8)$$

$$I_K = -g_K N_5^K (V - V_K) \quad (9)$$

$$I_{LVA} = -g_{LVA} N_6^{LVA} (V - V_{LVA}) \quad (10)$$

$$I_{BK} = -g_{BK} N_2^{BK} (V - V_{BK}) \quad (11)$$

$$I_{\text{Orco}} = -g_{\text{Orco}} \left(0.8 + 0.2 \sin\left(\frac{2\pi t}{24h}\right)\right) (V - V_{\text{Orco}}) \quad (12)$$

$$I_L = -g_L (V_L - V) \quad (13)$$

Here, g_χ is the maximal conductance, V is the membrane potential, and V_χ is the reversal potential for each ion current. The parameter values for each current can be found in Table 1.

Current	g_X (mS/cm^2)	V_X (mV)
I_L	4.3	-62.5
I_{LVA}	10.0	120
I_{NA}	29.17	45.0
I_K	12.96	-105.0
I_{BK}	9.0	-105.0
I_{ORCO}	5.0	0.0

Table 1. **Parameter values for model currents.**

Each transition rate $\alpha_k^{ion}(V)$ is calculated in the following way:

$$\alpha_k^{ion}(V) = \frac{p_{j(k)\infty}^{ion}(V)}{\tau_p(V)} \tag{14}$$

where $p_{j(k)\infty}^{ion}(V)$ is the steady state value of the specific gate that switches states in the destination state and $\tau_p(V)$ is the time constant of said gate. The steady state activation values and time constants for the LVA, Na, K, and BK channels were based on Viertel and Borisyuk (2019). The steady state functions for the activation gates are denoted with m_∞^{ion}, and those for the inactivation gates with h_∞^{ion}.

Each gate's steady state activation function, except for the BK channel, takes the form:

$$p_{j\infty}^{ion}(V) = \frac{1.0}{1.0 + \exp\left(\frac{(V-\theta_p)}{\beta_p}\right)} \tag{15}$$

The I_{BK} current is dependent on the intracellular calcium concentration and membrane potential as represented by the following equations:

$$m_\infty^{BK}(V) = \frac{1.0}{1.0 + \exp\left(\frac{\left(V - V_{\frac{1}{2}}\right)}{(-15.6)}\right)} \tag{16}$$

$$\frac{V_{\frac{1}{2}}}{2} = -20 + 59.2e^{-90[Ca]} + 96.7e^{-470[Ca]} \tag{17}$$

$$\tau_\alpha = -(q-1.0)\frac{(f-0.2)}{0.8} + 170 \tag{18}$$

$$q = 2.9 + 6.3e^{-360[Ca]} \tag{19}$$

$$s = -25.3 + 107.5e^{-120[ca]} \tag{20}$$

$$f = \frac{1.0}{10.0\left(e^{\frac{-(V+100.0-s)}{63.6}} + e^{\frac{(-150.0+(V+100.0-s))}{63.6}}\right)} \tag{21}$$

The intracellular concentration of calcium ions is described by the following equation:

$$\frac{d[Ca]}{dt} = -\gamma\frac{I_{LVA}}{zFd} + \frac{[Ca_0]-[Ca]}{\tau_{Ca}} \tag{22}$$

where Ca_0 is the steady state calcium concentration, γ describes calcium buffering, z is the ionic valence of calcium, F is Faraday's constant and d is the depth in microns at which calcium ions concentrate near the membrane.

The parameters of each steady state activation function as well as the time constant for each gating value can be found in Table 2.

Variable	θ	β	τ(ms)
m^{LVA}	-30	-4.8916	$\frac{40.0}{cosh\left(\frac{(V+37.1)}{9.7832}\right)}$
h^{LVA}	-59.2	11.2326	$\frac{350.0}{cosh\left(\frac{(V+59.2)}{22.4652}\right)}$
m^{Na}	-25.0	-6.5	0.2
h^{Na}	-26.0	9.0	$\frac{10.0}{cosh\left(\frac{(V+26.0)}{18.0}\right)}$
m^{K}	-26.0	-9.0	$\frac{10.0}{cosh\left(\frac{(V+26.0)}{18.0}\right)}$

Table 2. **Gating variable parameter values.**

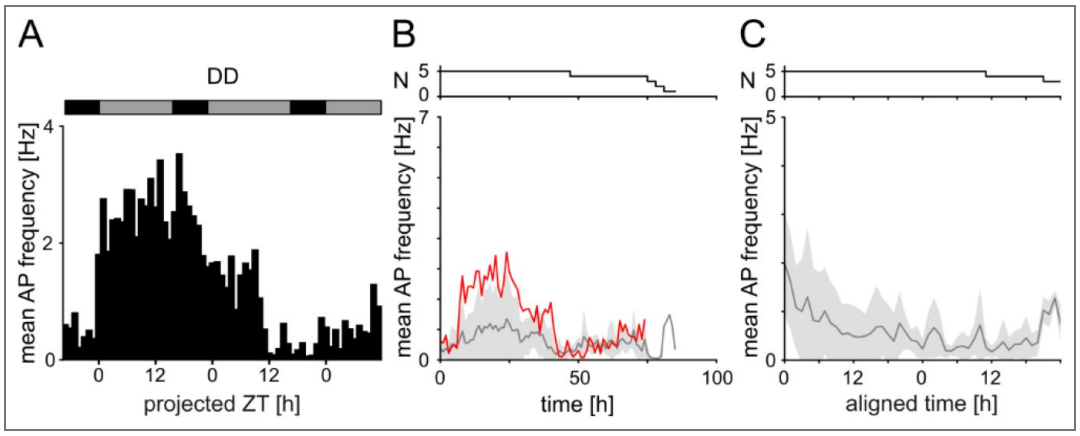

Figure 3 – Supplement. Spontaneous spiking activity of ORNs of pheromone-exposed male *M. sexta*. To enhance synchronization, males were exposed to females and pheromones as additional zeitgeber for 30 mins at ZT 16 before the start of the experiment. Recordings were obtained over multiple days in DD. **(A)** The spontaneous spike frequency of one long-term ORN recording in constant darkness (DD, the expected times of lights on are represented by grey bars above) **(B)** Mean spontaneous ORN spike frequency across all DD animals in 1 h bins. Data from the individual in **A** is highlighted in red. **(C)** Mean spontaneous ORN spike frequency across all DD animals in 1 h bins during the first 48 hours after aligning the time to the first maximum in spontaneous activity (see Methods). No circadian activity was evident in these pheromone-exposed males.

Data availability

The code for the mathematical ORN model presented in this paper is openly accessible at *https://github.com/a-c-schneider/VijayanForlinoEtAl2025_Model*

Acknowledgements

We thank Dr. Dieter Wicher (Max Planck Institute for Chemical Ecology, Jena, Germany) for generously providing OLC15, and Rishaban Radhakrishnan for help with Python codes. We thank Prof. Hülya Altuntaş for helpful discussions.

Additional information

Funding

AV, MF, YC, ACS, MEG, and MS were supported by Deutsche Forschungsgemeinschaft RTG 2749/1: “Biological Clocks on Multiple Time Scales”; KS and MS were supported by Deutsche Forschungsgemeinschaft STE531/20-2; PR was supported through the Add-on Fellowship for Interdisciplinary Life Science by the Joachim Herz Foundation.

Author contributions

Conceptualization: AV, MF, MEG, MS; data curation: AV, MF, YC, PR, KS, ACS, MEG, MS; formal analysis: AV, MF, YC, PD, ACS; funding acquisition: MEG, MS; investigation: AV, MF, YC, KS; methodology: MF, PR, MEG, MS; project administration: ACS, MEG, MS; resources: MEG, MS; software: AV, MF, PR, MEG; supervision: MEG, MS; validation: AV, MF, YC, PR, KS, ACS, MEG, MS; visualization: AV, MF, YC, ACS, MS; writing – original draft: AV, MF, ACS, MEG, MS; writing – reviewing & editing: AV, MF, YC, ACS, MEG, MS.

Funding

Funder	Grant reference number	Author
Deutsche Forschungsgemeinschaft (DFG)	RTG 2749/1	Mauro Forlino Martin E Garcia Aditi Vijayan Yajun Chang Monika Stengl Anna C Schneider
Deutsche Forschungsgemeinschaft (DFG)	STE531/20/2	Monika Stengl Katrin Schröder
Joachim Herz Stiftung (Joachim Herz Foundation)	Add-on Fellowship for Interdisciplinary Life Sciences	Pablo Rojas

Author ORCID iDs

Anna C Schneider: https://orcid.org/0000-0002-1270-836X
Monika Stengl: https://orcid.org/0000-0002-7896-872X

References

Bahk S, Jones WD (2016) Insect odorant receptor trafficking requires calmodulin. *BMC Biology* **14**:83 https://doi.org/10.1186/s12915-016-0306-x | PubMed

Baker TC, Vogt RG (1988) Measured Behavioural Latency in Response to Sex-Pheromone Loss in the Large Silk Moth Antheraea Polyphemus. *Journal of Experimental Biology* **137**:29-38 https://doi.org/10.1242/jeb.137.1.29 | PubMed

Baker TC, Willis MA, Haynes KF, Phelan PL (1985) A pulsed cloud of sex pheromone elicits upwind flight in male moths. *Physiological Entomology* **10**:257-265 https://doi.org/10.1111/j.1365-3032.1985.tb00045.x

Battelle B-A. (2013) What the Clock Tells the Eye: Lessons from an Ancient Arthropod. *Integrative and Comparative Biology* **53**:144-153 https://doi.org/10.1093/icb/ict020 | PubMed

Bau J, Justus KA, Cardé RT. (2002) Antennal resolution of pulsed pheromone plumes in three moth species. *Journal of Insect Physiology* **48**:433-442 https://doi.org/10.1016/S0022-1910(02)00062-8 | PubMed

Bau J, Justus KA, Loudon C, Cardé RT. (2005) Electroantennographic Resolution of Pulsed Pheromone Plumes in Two Species of Moths with Bipectinate Antennae. *Chemical Senses* **30**:771-780 https://doi.org/10.1093/chemse/bji069 | PubMed

Bell RA, Joachim FG (1976) Techniques for Rearing Laboratory Colonies of Tobacco Hornworms and Pink Bollworms1. *Annals of the Entomological Society of America* **69**:365-373 https://doi.org/10.1093/aesa/69.2.365

Benton R, Sachse S, Michnick SW, Vosshall LB (2006) Atypical Membrane Topology and Heteromeric Function of Drosophila Odorant Receptors In Vivo. *PLOS Biology* **4**:e20 https://doi.org/10.1371/journal.pbio.0040020 | PubMed

Boekhoff I, Seifert E, Göggerle S, Lindemann M, Krüger B-W, Breer H. (1993) Pheromone-induced second-messenger signaling in insect antennae. *Insect Biochemistry and Molecular Biology* **23**:757-762 https://doi.org/10.1016/0965-1748(93)90063-X

Bose A, Golowasch J, Guan Y, Nadim F. (2014) The role of linear and voltage-dependent ionic currents in the generation of slow wave oscillations. *Journal of Computational Neuroscience* **37**:229-242 https://doi.org/10.1007/s10827-014-0498-4 | PubMed

Butterwick JA, Mármol J, Kim KH, Kahlson MA, Rogow JA, Walz T, Ruta V. (2018) Cryo-EM structure of the insect olfactory receptor Orco. *Nature* **560**:447-452 https://doi.org/10.1038/s41586-018-0420-8 | PubMed

Cao L-H, Jing B-Y, Yang D, Zeng X, Shen Y, Tu Y, Luo D-G. (2016) Distinct signaling of Drosophila chemoreceptors in olfactory sensory neurons. *Proceedings of the National Academy of Sciences* **113**:E902-E911 https://doi.org/10.1073/pnas.1518329113 | PubMed

Chen S, Luetje CW (2012) Identification of New Agonists and Antagonists of the Insect Odorant Receptor Co-Receptor Subunit. *PLOS One* **7**:e36784 https://doi.org/10.1371/journal.pone.0036784 | PubMed

Cochet-Bissuel M, Lory P, Monteil A. (2014) The sodium leak channel, NALCN, in health and disease. *Frontiers in Cellular Neuroscience* **8**:132 https://doi.org/10.3389/fncel.2014.00132 | PubMed

Dacks AM, Dacks JB, Christensen TA, Nighorn AJ (2006) The cloning of one putative octopamine receptor and two putative serotonin receptors from the tobacco hawkmoth, Manduca sexta. *Insect Biochemistry and Molecular Biology* **36**:741-747 https://doi.org/10.1016/j.ibmb.2006.07.002 | PubMed

Das A, Holmes TC, Sheeba V. (2016) dTRPA1 in Non-circadian Neurons Modulates Temperature-dependent Rhythmic Activity in Drosophila melanogaster. *Journal of Biological Rhythms* **31**:272-288 https://doi.org/10.1177/0748730415627037 | PubMed

Dolzer J, Fischer K, Stengl M. (2003) Adaptation in pheromone-sensitive trichoid sensilla of the hawkmoth Manduca sexta. *Journal of Experimental Biology* **206**:1575-1588 https://doi.org/10.1242/jeb.00302 | PubMed

Dolzer J, Krannich S, Fischer K, Stengl M. (2001) Oscillations of the Transepithelial Potential of Moth Olfactory Sensilla Are Influenced by Octopamine and Serotonin. *Journal of Experimental Biology* **204**:2781-2794 https://doi.org/10.1242/jeb.204.16.2781 | PubMed

Dolzer J, Krannich S, Stengl M. (2008) Pharmacological Investigation of Protein Kinase C- and cGMP-Dependent Ion Channels in Cultured Olfactory Receptor Neurons of the Hawkmoth Manduca sexta. *Chemical Senses* **33**:803-813 https://doi.org/10.1093/chemse/bjn043 | PubMed

Dolzer J, Schröder K, Stengl M. (2021) Cyclic nucleotide-dependent ionic currents in olfactory receptor neurons of the hawkmoth Manduca sexta suggest pull–push sensitivity modulation. *European Journal of Neuroscience* **54**:4804-4826 https://doi.org/10.1111/ejn.15346 | PubMed

Dubowy C, Sehgal A. (2017) Circadian Rhythms and Sleep in Drosophila melanogaster. *Genetics* **205**:1373-1397 https://doi.org/10.1534/genetics.115.185157 | PubMed

Edgar RS, Green EW, Zhao Y, van Ooijen G, Olmedo M, Qin X, Xu Y, Pan M, Valekunja UK, Feeney KA, *et al.* (2012) Peroxiredoxins are conserved markers of circadian rhythms. *Nature* **485**:459-464 https://doi.org/10.1038/nature11088 | PubMed

Fandino RA, Haverkamp A, Bisch-Knaden S, Zhang J, Bucks S, Nguyen TAT, Schröder K, Werckenthin A, Rybak J, Stengl M, *et al.* (2019) Mutagenesis of odorant coreceptor Orco fully disrupts foraging but not oviposition behaviors in the hawkmoth Manduca sexta. *Proceedings of the National Academy of Sciences* **116**:15677-15685 https://doi.org/10.1073/pnas.1902089116 | PubMed

Flecke C, Dolzer J, Krannich S, Stengl M. (2006) Perfusion with cGMP analogue adapts the action potential response of pheromone-sensitive sensilla trichoidea of the hawkmoth Manduca sexta in a daytime-dependent manner. *Journal of Experimental Biology* **209**:3898-3912 https://doi.org/10.1242/jeb.02432 | PubMed

Flecke C, Nolte A, Stengl M. (2010) Perfusion with cAMP analogue affects pheromone-sensitive trichoid sensilla of the hawkmoth Manduca sexta in a time-dependent manner. *Journal of Experimental Biology* **213**:842-852 https://doi.org/10.1242/jeb.032839 | PubMed

Flecke C, Stengl M. (2009) Octopamine and tyramine modulate pheromone-sensitive olfactory sensilla of the hawkmoth Manduca sexta in a time-dependent manner. *Journal of Comparative Physiology A* **195**:529-545 https://doi.org/10.1007/s00359-009-0429-4 | PubMed

Forlino M, Vijayan A, Schneider AC, Stengl M, Garcia ME (2025) ORN-Orco-Model. https://github.com/a-c-schneider/VijayanForlinoEtAl2025_Model

Fox RF, Lu Y. (1994) Emergent collective behavior in large numbers of globally coupled independently stochastic ion channels. *Physical Review E* **49**:3421-3431 https://doi.org/10.1103/PhysRevE.49.3421 | PubMed

Gawalek P, Stengl M. (2018) The Diacylglycerol Analogs OAG and DOG Differentially Affect Primary Events of Pheromone Transduction in the Hawkmoth Manduca sexta in a Zeitgebertime-Dependent Manner Apparently Targeting TRP Channels. *Frontiers in Cellular Neuroscience* **12**:218 https://doi.org/10.3389/fncel.2018.00218 | PubMed

Géron A, Werner Johannes, Wattiez Ruddy, Matallana-Surget S. (2024) Towards the discovery of novel molecular clocks in Prokaryotes. *Critical Reviews in Microbiology* **50**:491-503 https://doi.org/10.1080/1040841X.2023.2220789 | PubMed

Getahun MN, Olsson SB, Lavista-Llanos S, Hansson BS, Wicher D. (2013) Insect Odorant Response Sensitivity Is Tuned by Metabotropically Autoregulated Olfactory Receptors. *PLOS One* **8**:e58889 https://doi.org/10.1371/journal.pone.0058889 | PubMed

Getahun MN, Thoma M, Lavista-Llanos S, Keesey I, Fandino RA, Knaden M, Wicher D, Olsson SB, Hansson BS (2016) Intracellular regulation of the insect chemoreceptor complex impacts odour localization in flying insects. *Journal of Experimental Biology* **219**:3428-3438 https://doi.org/10.1242/jeb.143396 | PubMed

Ghosh S, Suray C, Bozzolan F, Palazzo A, Monsempès C, Lecouvreur F, Chatterjee A. (2024) Pheromone-mediated command from the female to male clock induces and synchronizes circadian rhythms of the moth Spodoptera littoralis. *Current biology* **34**:1414-1425.e5. https://doi.org/10.1016/j.cub.2024.02.042 | PubMed

Goldstein SAN, Bockenhauer D, O'Kelly I, Zilberberg N. (2001) Potassium leak channels and the KCNK family of two-p-domain subunits. *Nature Reviews Neuroscience* **2**:175-184 https://doi.org/10.1038/35058574 | PubMed

Golowasch J, Bose A, Guan Y, Salloum D, Roeser A, Nadim F. (2017) A balance of outward and linear inward ionic currents is required for generation of slow-wave oscillations. *Journal of Neurophysiology* **118**:1092-1104 https://doi.org/10.1152/jn.00240.2017 | PubMed

Guo H, Smith DP (2022) Time-Dependent Odorant Sensitivity Modulation in Insects. *Insects* **13**:354 https://doi.org/10.3390/insects13040354 | PubMed

Guo H, Smith DP (2017) Odorant Receptor Desensitization in Insects. *Journal of Experimental Neuroscience* **11**:1179069517748600 https://doi.org/10.1177/1179069517748600 | PubMed

Hall JC, Rosbash M. (1993) Oscillating molecules and how they move circadian clocks across evolutionary boundaries. *Proceedings of the National Academy of Sciences of the United States of America* **90**:5382-5383 PubMed | https://doi.org/10.1073/pnas.90.12.5382

Halls ML, Cooper DMF (2011) Regulation by Ca2+-Signaling Pathways of Adenylyl Cyclases. *Cold Spring Harbor Perspectives in Biology* **3**:a004143 https://doi.org/10.1101/cshperspect.a004143 | PubMed

Hardin PE (2011) Molecular Genetic Analysis of Circadian Timekeeping in Drosophila. In: Brody S (Ed). *Advances in Genetics, The Genetics of Circadian Rhythms* Academic Press. pp. 141-173 https://doi.org/10.1016/B978-0-12-387690-4.00005-2 | PubMed

Hastings MH, Smyllie NJ, Patton AP (2020) Molecular-genetic Manipulation of the Suprachiasmatic Nucleus Circadian Clock. *Journal of Molecular Biology* **432**:3639-3660 https://doi.org/10.1016/j.jmb.2020.01.019 | PubMed

Hille B. (2001) *Ion Channels of Excitable Membranes, Third Edition, Third Edition* Oxford University Press.

Itagaki H, Conner WE (1988) Calling Behavior of Manduca sexta (L.) (Lepidoptera: Sphingidae) with Notes on the Morphology of the Female Sex Pheromone Gland. *Annals of the Entomological Society of America* **81**:798-807 https://doi.org/10.1093/aesa/81.5.798

Jain K, Lavista-Llanos S, Grabe V, Hansson BS, Wicher D. (2021) Calmodulin regulates the olfactory performance in Drosophila melanogaster. *Scientific Reports* **11**:3747 https://doi.org/10.1038/s41598-021-83296-9 | PubMed

Jones PL, Pask GM, Rinker DC, Zwiebel LJ (2011) Functional agonism of insect odorant receptor ion channels. *Proceedings of the National Academy of Sciences* **108**:8821-8825 https://doi.org/10.1073/pnas.1102425108 | PubMed

Kaissling KE, Hildebrand JG, Tumlinson JH (1989) Pheromone receptor cells in the male moth Manduca sexta. *Archives of Insect Biochemistry and Physiology* **10**:273-279 https://doi.org/10.1002/arch.940100403

Kaissling KE, Thorson J. (1980) Insect Olfactory Sensilla: Structural, Chemical and Electrical Aspects of the Functional Organisation. In: Sattelle DB, Hall LM, Hildebrand JG (Eds). *Receptors for Neurotransmitters, Hormones and Pheromones in Insects* Elsevier/North-Holland Biomedical Press. pp. 261-282

Kaissling KE, Zack Strausfeld C, Rumbo ER (1987) Adaptation processes in insect olfactory receptors. Mechanisms and behavioral significance. *Annals of the New York Academy of Sciences* **510**:104-112 https://doi.org/10.1111/j.1749-6632.1987.tb43475.x | PubMed

Kalinová B, Hoskovec M, Liblikas I, Unelius CR, Hansson BS (2001) Detection of Sex Pheromone Components in Manduca sexta (L.). *Chemical Senses* **26**:1175-1186 https://doi.org/10.1093/chemse/26.9.1175 | PubMed

Kodirov SA (2022) Probability that there is a mammalian counterpart of cardiac clock in insects.Archives of Insect Biochemistry and Physiology. *Archives of insect biochemistry and physiology* **110**:e21867 https://doi.org/10.1002/arch.21867 | PubMed

Krishnan B, Dryer SE, Hardin PE (1999) Circadian rhythms in olfactory responses of Drosophila melanogaster. *Nature* **400**:375-378 https://doi.org/10.1038/22566 | PubMed

Lamont EW, Amir S. (2010) Circadian and Ultradian Clocks/Rhythms. In: Koob GF, Moal ML, Thompson RF (Eds). *Encyclopedia of Behavioral Neuroscience* Academic Press. pp. 257-261 https://doi.org/10.1016/B978-0-08-045396-5.00223-2

Lee C-H, MacKinnon R. (2017) Structures of the Human HCN1 Hyperpolarization-Activated Channel. *Cell* **168**:111-120.e11. https://doi.org/10.1016/j.cell.2016.12.023 | PubMed

Lee JK, Strausfeld NJ (1990) Structure, distribution and number of surface sensilla and their receptor cells on the olfactory appendage of the male mothManduca sexta. *Journal of Neurocytology* **19**:519-538 https://doi.org/10.1007/BF01257241 | PubMed

Liu JS, Passaglia CL (2011) Spike firing pattern of output neurons of the Limulus circadian clock. *Journal of Biological Rhythms* **26**:335-344 https://doi.org/10.1177/0748730411409712 | PubMed

Livak KJ, Schmittgen TD (2001) Analysis of relative gene expression data using real-time quantitative PCR and the 2-ΔΔ C(T) Method. *Methods* **25**:402-408 https://doi.org/10.1006/meth.2001.1262 | PubMed

Lüthi A, McCormick DA (1998) H-Current: Properties of a Neuronal and Network Pacemaker. *Neuron* **21**:9-12 https://doi.org/10.1016/S0896-6273(00)80509-7

Mandala VS, Fu Z, MacKinnon R. (2025) Molecular contacts in self-assembling clusters of membrane proteins. *Proceedings of the National Academy of Sciences* **122**:e2507112122 https://doi.org/10.1073/pnas.2507112122 | PubMed

Marion-Poll F, Tobin TR (1992) Temporal coding of pheromone pulses and trains in Manduca sexta. *Journal of Comparative Physiology A* **171**:505-512 https://doi.org/10.1007/BF00194583 | PubMed

Martín F, Charro M, Alcorta E. (2001) Mutations affecting the cAMP transduction pathway modify olfaction in Drosophila. *Journal of Comparative Physiology A* **187**:359-370 https://doi.org/10.1007/s003590100208 | PubMed

Merlin C, François M-C, Queguiner I, Maïbèche-Coisné M, Jacquin-Joly E. (2006) Evidence for a putative antennal clock in Mamestra brassicae: Molecular cloning and characterization of two clock genes –period and cryptochrome– in antennae. *Insect Molecular Biology* **15**:137-145 https://doi.org/10.1111/j.1365-2583.2006.00617.x | PubMed

Merlin C, Gegear RJ, Reppert SM (2009) Antennal Circadian Clocks Coordinate Sun Compass Orientation in Migratory Monarch Butterflies. *Science* **325**:1700-1704 https://doi.org/10.1126/science.1176221 | PubMed

Merlin C, Lucas P, Rochat D, François M-C, Maïbèche-Coisne M, Jacquin-Joly E. (2007) An Antennal Circadian Clock and Circadian Rhythms in Peripheral Pheromone Reception in the Moth Spodoptera littoralis. *Journal of Biological Rhythms* **22**:502-514 https://doi.org/10.1177/0748730407307737 | PubMed

Millar AJ (2016) The Intracellular Dynamics of Circadian Clocks Reach for the Light of Ecology and Evolution. *Annual Review of Plant Biology* **67**:595-618 https://doi.org/10.1146/annurev-arplant-043014-115619 | PubMed

Mönke G, Sorgenfrei FA, Schmal C, Granada AE (2020) Optimal time frequency analysis for biological data - pyBOAT. *bioRxiv* https://doi.org/10.1101/2020.04.29.067744

Mukunda L, Miazzi F, Kaltofen S, Hansson BS, Wicher D. (2014) Calmodulin modulates insect odorant receptor function. *Cell Calcium* **55**:191-199 https://doi.org/10.1016/j.ceca.2014.02.013 | PubMed

Mukunda L, Miazzi F, Sargsyan V, Hansson BS, Wicher D. (2016) Calmodulin Affects Sensitization of Drosophila melanogaster Odorant Receptors. *Frontiers in Cellular Neuroscience* **10** https://doi.org/10.3389/fncel.2016.00028 | PubMed

Nakagawa T, Vosshall LB (2009) Controversy and consensus: noncanonical signaling mechanisms in the insect olfactory system. *Current Opinion in Neurobiology* **19**:284-292 https://doi.org/10.1016/j.conb.2009.07.015 | PubMed

Nishiitsutsuji-Uwo J, Pittendrigh CS (1968) Central nervous system control of circadian rhythmicity in the cockroach II. The pathway of light signals that entrain the rhythm. *Zeitschrift für vergleichende Physiologie* **58**:1-13 https://doi.org/10.1007/BF00302433

Nolte A, Funk NW, Mukunda L, Gawalek P, Werckenthin A, Hansson BS, Wicher D, Stengl M. (2013) In situ Tip-Recordings Found No Evidence for an Orco-Based Ionotropic Mechanism of Pheromone-Transduction in Manduca sexta. *PLOS One* **8**:e62648 https://doi.org/10.1371/journal.pone.0062648 | PubMed

Nolte A, Gawalek P, Koerte S, Wei H, Schumann R, Werckenthin A, Krieger J, Stengl M. (2016) No Evidence for Ionotropic Pheromone Transduction in the Hawkmoth Manduca sexta. *PLOS One* **11**:e0166060 https://doi.org/10.1371/journal.pone.0166060 | PubMed

O'Neill JS, Reddy AB (2011) Circadian clocks in human red blood cells. *Nature* **469**:498-503 https://doi.org/10.1038/nature09702 | PubMed

Ono D, Huan Wang, Hung CJ, Hsin-tzu Wang, Kon N, Yamanaka A, Li Y, Sugiyama T. (2023) Network-driven intracellular cAMP coordinates circadian rhythm in the suprachiasmatic nucleus. *Science Advances* **9**:eabq7032 https://doi.org/10.1126/sciadv.abq7032 | PubMed

Page TL, Koelling E. (2003) Circadian rhythm in olfactory response in the antennae controlled by the optic lobe in the cockroach. *Journal of Insect Physiology* **49**:697-707 https://doi.org/10.1016/s0022-1910(03)00071-4 | PubMed

Pask GM, Bobkov YV, Corey EA, Ache BW, Zwiebel LJ (2013) Blockade of Insect Odorant Receptor Currents by Amiloride Derivatives. *Chemical Senses* **38**:221-229 https://doi.org/10.1093/chemse/bjs100 | PubMed

Patel AJ, Honoré E. (2001) Properties and modulation of mammalian 2P domain K+ channels. *Trends in Neurosciences* **24**:339-346 https://doi.org/10.1016/S0166-2236(00)01810-5 | PubMed

Pézier A, Acquistapace A, Renou M, Rospars J-P, Lucas P. (2007) Ca2+ Stabilizes the Membrane Potential of Moth Olfactory Receptor Neurons at Rest and Is Essential for Their Fast Repolarization. *Chemical Senses* **32**:305-317 https://doi.org/10.1093/chemse/bjl059 | PubMed

Plautz JD, Kaneko M, Hall JC, Kay SA (1997) Independent Photoreceptive Circadian Clocks Throughout Drosophila. *Science* **278**:1632-1635 https://doi.org/10.1126/science.278.5343.1632 | PubMed

Prosser RA, Gillette MU (1991) Cyclic changes in cAMP concentration and phosphodiesterase activity in a mammalian circadian clock studied in vitro. *Brain Research* **568**:185-192 https://doi.org/10.1016/0006-8993(91)91396-I | PubMed

Prosser RA, McArthur AJ, Gillette MU (1989) cGMP induces phase shifts of a mammalian circadian pacemaker at night, in antiphase to cAMP effects. *Proceedings of the National Academy of Sciences of the United States of America* **86**:6812-6815 PubMed | https://doi.org/10.1073/pnas.86.17.6812

Pu S, Thomas PJ (2020) Fast and Accurate Langevin Simulations of Stochastic Hodgkin-Huxley Dynamics. *Neural Computation* **32**:1775-1835 https://doi.org/10.1162/neco_a_01312 | PubMed

Ratliff J, Franci A, Marder E, O'Leary T. (2021) Neuronal oscillator robustness to multiple global perturbations. *Biophysical Journal* **120**:1454-1468 https://doi.org/10.1016/j.bpj.2021.01.038 | PubMed

Redkozubov A. (2000) Guanosine 3',5'-Cyclic Monophosphate Reduces the Response of the Moth's Olfactory Receptor Neuron to Pheromone. *Chemical Senses* **25**:381-385 https://doi.org/10.1093/chemse/25.4.381 | PubMed

Reinhard N, Fukuda A, Manoli G, Derksen E, Saito A, Möller G, Sekiguchi M, Rieger D, Helfrich-Förster C, Yoshii T, *et al.* (2024) Synaptic connectome of the Drosophila circadian clock. *Nature Communications* **15**:10392 https://doi.org/10.1038/s41467-024-54694-0 | PubMed

Riffell JA, Abrell L, Hildebrand JG (2008) Physical processes and real-time chemical measurement of the insect olfactory environment. *Journal of Chemical Ecology* **34**:837-853 https://doi.org/10.1007/s10886-008-9490-7 | PubMed

Robinson RB, Siegelbaum SA (2003) Hyperpolarization-activated cation currents: from molecules to physiological function. *Annual Review of Physiology* **65**:453-480 https://doi.org/10.1146/annurev.physiol.65.092101.142734 | PubMed

Sargsyan V, Getahun MN, Lavista Llanos S, Olsson SB, Hansson BS, Wicher D. (2011) Phosphorylation via PKC Regulates the Function of the Drosophila Odorant Co-Receptor. *Frontiers in Cellular Neuroscience* **5** https://doi.org/10.3389/fncel.2011.00005 | PubMed

Sato K, Pellegrino M, Takao Nakagawa, Tatsuro Nakagawa, Vosshall LB, Touhara K. (2008) Insect olfactory receptors are heteromeric ligand-gated ion channels. *Nature* **452**:1002-1006 https://doi.org/10.1038/nature06850 | PubMed

Sauman I, Reppert SM (1998) Brain Control of Embryonic Circadian Rhythms in the Silkmoth Antheraea pernyi. *Neuron* **20**:741-748 https://doi.org/10.1016/S0896-6273(00)81012-0 | PubMed

Schendzielorz J, Schendzielorz T, Arendt A, Stengl M. (2014) Bimodal Oscillations of Cyclic Nucleotide Concentrations in the Circadian System of the Madeira Cockroach Rhyparobia maderae. *Journal of Biological Rhythms* **29**:318-331 https://doi.org/10.1177/0748730414546133 | PubMed

Schendzielorz T, Peters W, Boekhoff I, Stengl M. (2012) Time of Day Changes in Cyclic Nucleotides Are Modified via Octopamine and Pheromone in Antennae of the Madeira Cockroach. *Journal of Biological Rhythms* **27**:388-397 https://doi.org/10.1177/0748730412456265 | PubMed

Schendzielorz T, Schirmer K, Stolte P, Stengl M. (2015) Octopamine Regulates Antennal Sensory Neurons via Daytime-Dependent Changes in cAMP and IP_3 Levels in the Hawkmoth Manduca sexta. *PLOS One* **10**:e0121230 https://doi.org/10.1371/journal.pone.0121230 | PubMed

Schmidt DR, Galán RF, Thomas PJ (2018) Stochastic shielding and edge importance for Markov chains with timescale separation. *PLOS Computational Biology* **14**:e1006206 https://doi.org/10.1371/journal.pcbi.1006206 | PubMed

Schmidt DR, Thomas PJ (2014) Measuring Edge Importance: A Quantitative Analysis of the Stochastic Shielding Approximation for Random Processes on Graphs. *The Journal of Mathematical Neuroscience* **4**:6 https://doi.org/10.1186/2190-8567-4-6 | PubMed

Schneider AC, Schröder K, Chang Y, Nolte A, Gawalek P, Stengl M. (2025) Hawkmoth Pheromone Transduction Involves G-Protein–Dependent Phospholipase Cβ Signaling. *eNeuro* **12**:ENEURO.0376-24.2024 https://doi.org/10.1523/ENEURO.0376-24.2024 | PubMed

Schuckel J, Siwicki KK, Stengl M. (2007) Putative circadian pacemaker cells in the antenna of the hawkmoth Manduca sexta. *Cell and Tissue Research* **330**:271-278 https://doi.org/10.1007/s00441-007-0471-x | PubMed

Schweitzer ES, Sanes JR, Hildebrand JG (1976) Ontogeny of electroantennogram responses in the moth, Manduca sexta. *Journal of Insect Physiology* **22**:955-960 https://doi.org/10.1016/0022-1910(76)90078-0

Sharma A, Rahman G, Gorelik J, Bhargava A. (2023) Voltage-Gated T-Type Calcium Channel Modulation by Kinases and Phosphatases: The Old Ones, the New Ones, and the Missing Ones. *Cells* **12**:461 https://doi.org/10.3390/cells12030461 | PubMed

Silvegren G, Löfstedt C, Qi Rosén W. (2005) Circadian mating activity and effect of pheromone pre-exposure on pheromone response rhythms in the moth Spodoptera littoralis. *Journal of Insect Physiology* **51**:277-286 https://doi.org/10.1016/j.jinsphys.2004.11.013 | PubMed

Steinbrecht RA (1992) Experimental morphology of insect olfaction: Tracer studies, x-ray microanalysis, autoradiography, and immunocytochemistry with silkmoth antennae. *Microscopy Research and Technique* **22**:336-350 https://doi.org/10.1002/jemt.1070220404 | PubMed

Stengl M. (2010) Pheromone Transduction in Moths. *Frontiers in Cellular Neuroscience* **4**:133 https://doi.org/10.3389/fncel.2010.00133 | PubMed

Stengl M. (1994) Inositol-trisphosphate-dependent calcium currents precede cation currents in insect olfactory receptor neurons in vitro. *Journal of Comparative Physiology A* **174**:187-194 https://doi.org/10.1007/BF00193785 | PubMed

Stengl M. (1993) Intracellular-Messenger-Mediated Cation Channels in Cultured Olfactory Receptor Neurons. *Journal of Experimental Biology* **178**:125-147 https://doi.org/10.1242/jeb.178.1.125 | PubMed

Stengl M, Funk NW (2013) The role of the coreceptor Orco in insect olfactory transduction. *Journal of Comparative Physiology A* **199**:897-909 https://doi.org/10.1007/s00359-013-0837-3 | PubMed

Stengl M, Schneider AC (2024) Contribution of membrane-associated oscillators to biological timing at different timescales. *Frontiers in Physiology* **14**:1243455 https://doi.org/10.3389/fphys.2023.1243455 | PubMed

Stengl M, Schröder K. (2021) 14 - Multiscale timing of pheromone transduction in hawkmoth olfactory receptor neurons. In: Blomquist GJ, Vogt RG (Eds). *Insect PheromoneBiochemistry and Molecular Biology (Second Edition)* Academic Press. pp. 435-468 https://doi.org/10.1016/B978-0-12-819628-1.00014-6

Stengl M, Zintl R, De Vente J, Nighorn A. (2001) Localization of cGMP immunoreactivity and of soluble guanylyl cyclase in antennal sensilla of the hawkmoth Manduca sexta. *Cell and Tissue Research* **304**:409-421 https://doi.org/10.1007/s004410000336 | PubMed

Szyszka P, Gerkin RC, Galizia CG, Smith BH (2014) High-speed odor transduction and pulse tracking by insect olfactory receptor neurons. *Proceedings of the National Academy of Sciences* **111**:16925-16930 https://doi.org/10.1073/pnas.1412051111 | PubMed

Talley EM, Solórzano G, Lei Q, Kim D, Bayliss DA (2001) CNS Distribution of Members of the Two-Pore-Domain (KCNK) Potassium Channel Family. *Journal of Neuroscience* **21**:7491-7505 https://doi.org/10.1523/JNEUROSCI.21-19-07491.2001 | PubMed

Tanoue S, Krishnan P, Krishnan B, Dryer SE, Hardin PE (2004) Circadian Clocks in Antennal Neurons Are Necessary and Sufficient for Olfaction Rhythms in Drosophila. *Current Biology* **14**:638-649 https://doi.org/10.1016/j.cub.2004.04.009 | PubMed

Thaben PF, Westermark PO (2014) Detecting Rhythms in Time Series with RAIN. *Journal of Biological Rhythms* **29**:391-400 https://doi.org/10.1177/0748730414553029 | PubMed

Thaiss CA, Zeevi D, Levy M, Zilberman-Schapira G, Suez J, Tengeler AC, Abramson L, Katz MN, Korem T, Zmora N, *et al.* (2014) Transkingdom Control of Microbiota Diurnal Oscillations Promotes Metabolic Homeostasis. *Cell* **159**:514-529 https://doi.org/10.1016/j.cell.2014.09.048 | PubMed

Tripathy S, Staudacher EM, Peters O, Kalwar F, Hatfield M, Daly K. (2010) Odors pulsed at wing beat frequencies are tracked by primary olfactory networks and enhance odor detection. *Frontiers in Cellular Neuroscience* **4** https://doi.org/10.3389/neuro.03.001.2010 | PubMed

Viertel R, Borisyuk A. (2019) A Computational model of the mammalian external tufted cell. *Journal of Theoretical Biology* **462**:109-121 https://doi.org/10.1016/j.jtbi.2018.10.003 | PubMed

Wicher D. (2018) Tuning Insect Odorant Receptors. *Frontiers in Cellular Neuroscience* **12**:94 https://doi.org/10.3389/fncel.2018.00094 | PubMed

Wicher D, Miazzi F. (2021) Functional properties of insect olfactory receptors: ionotropic receptors and odorant receptors. *Cell and Tissue Research* **383**:7-19 https://doi.org/10.1007/s00441-020-03363-x | PubMed

Wicher D, Schäfer R, Bauernfeind R, Stensmyr MC, Heller R, Heinemann SH, Hansson BS (2008) Drosophila odorant receptors are both ligand-gated and cyclic-nucleotide-activated cation channels. *Nature* **452**:1007-1011 https://doi.org/10.1038/nature06861 | PubMed

Zhou X, Yuan C, Guo A. (2005) Drosophila Olfactory Response Rhythms Require Clock Genes but Not Pigment Dispersing Factor or Lateral Neurons. *Journal of Biological Rhythms* **20**:237-244 https://doi.org/10.1177/0748730405274451 | PubMed

Ziegelberger G, van den Berg M, Kaissling KE, Klumpp S, Schultz JE (1990) Cyclic GMP levels and guanylate cyclase activity in pheromone-sensitive antennae of the silkmoths Antheraea polyphemus and Bombyx mori. *Journal of Neuroscience* **10**:1217-1225 https://doi.org/10.1523/JNEUROSCI.10-04-01217.1990 | PubMed

Peer reviews

Joint Public Review:

This manuscript puts forward the provocative idea that a posttranslational feedback loop regulates daily and ultradian rhythms in neuronal excitability. The authors used in vivo long-term tip recordings of the long trichoid sensilla of male hawkmoths to analyze spontaneous spiking activity indicative of the ORNs' endogenous membrane potential oscillations. This firing pattern was disrupted by pharmacological blockade of the Orco receptor. They then use these recordings together with computational modeling to predict that Orco receptor neuron (ORN) activity is required for circadian, not ultradian, firing patterns. Orco did not show a circadian expression pattern in a qPCR experiment, and its conductance was proposed to be regulated by cyclic nucleotide levels. This evidence led the authors to conclude that a post-translational feedback loop (PTFL) clockwork, associated with the ORN plasma membrane, allows for temporal control of pheromone detection via the generation of multi-scale endogenous membrane potential oscillations. The findings will interest researchers in neurophysiology, circadian rhythms, and sensory biology. However, the manuscript has limited experimental evidence to support its central hypothesis and is undermined by several assumptions that underlie their data analysis and model builds, as well as insufficient

biological data including critical controls to validate and/or fully justify the model the authors are proposing.

Strengths:

The authors raise several intriguing model-based hypotheses regarding the mechanisms that underlie the generation of olfactory rhythms. The electrophysiological approach and the long-term recording paradigm are elegant and technically impressive. In the revised version, the authors have added additional qPCR data supporting the lack of rhythmic Orco transcript expression and included a new figure suggesting that cAMP can modulate Orco conductance.

Major weaknesses:

(1) The cAMP experiment was only conducted at one time-point, which is insufficient to support the central claim that "AMP and cGMP may have ZT-dependent effects on Orco conductivity".

(2) The revised manuscript continues to rely heavily on prior publications or defers key mechanistic questions (or important manipulations) to future studies. In its current form, the evidence presented remains insufficient to support the central claim that a PTFL constitutes the primary underlying circadian clock mechanism. The proposed model is intriguing, but the data provided do not yet directly demonstrate the novel mechanism.

https://doi.org/10.7554/eLife.108100.2.sa1

Author response:

The following is the authors' response to the original reviews.

> ***Joint Public Review***
>
> *This manuscript puts forward the provocative idea that a posttranslational feedback loop regulates daily and ultradian rhythms in neuronal excitability. The authors used in vivo long-term tip recordings of the long trichoid sensilla of male hawkmoths to analyze spontaneous spiking activity indicative of the ORNs' endogenous membrane potential oscillations. This firing pattern was disrupted by pharmacological blockade of the Orco receptor. They then use these recordings together with computational modeling to predict that Orco receptor neuron (ORN) activity is required for circadian, not ultradian, firing patterns. Orco did not show a circadian expression pattern in a qPCR experiment, and its conductance was proposed to be regulated by cyclic nucleotide levels. This evidence led the authors to conclude that a post-translational feedback loop (PTFL) clockwork, associated with the ORN plasma membrane, allows for temporal control of pheromone detection via the generation of multi-scale endogenous membrane potential oscillations. The findings will interest researchers in neurophysiology, circadian rhythms, and sensory biology. However, the manuscript has limited experimental evidence to support its central hypothesis and is undermined by several questionable assumptions that underlie their data analysis and model builds, as well as insufficient biological data, including critical controls to validate and/or fully justify the model the authors are proposing.*

We thank the reviewers for their thorough and thoughtful comments and believe that the manuscript is much stronger now after the revision which incorporates the requested changes. We added results of new experiments and additional analyses. Although these new insights did not change the previous conclusions, we significantly reworked the Discussion and added further references to clarify the conclusions we want to make.

Please note that we used ORN as acronym for “olfactory receptor neuron” throughout the manuscript. ORNs contain odorant receptors (ORs), and in insects these ORs associate with the olfactory receptor co-receptor (Orco) to be trafficked to the membrane of the cilium of the ORN, where they can be contacted by pheromones and odorants. In *Manduca sexta*, evidence is accumulating for G-protein coupled metabotropic pheromone transduction and not for OR-Orco dependent ionotropic transduction, as shown for *Drosophila melanogaster*. In both insect species, besides its chaperone function, Orco can form leaky cation channels, which can regulate the spontaneous spiking activity of ORNs. In this study, we explored this role of Orco.

> *Strengths:*
>
> *The study is notable for its combination of long-term in vivo tip recordings with computational modeling, which is technically challenging and adds weight to the authors' claims. The link between Orco, cyclic nucleotides, and circadian regulation is potentially important for sensory neuroscience, and the modeling framework itself - a stochastic Hodgkin-Huxley formulation that explicitly incorporates channel noise - is a solid and forward-looking contribution. Together, these elements make the study conceptually bold and of clear interest to circadian and olfactory biologists.*
>
> *Major weaknesses:*
>
> *At the same time, several limitations temper the conclusions. The pharmacological evidence relies on a single antagonist and concentration, without key controls. The circadian analysis is based on relatively small numbers of neurons, with rhythms detected only in subsets, and the alignment procedure used in constant darkness raises concerns of bias. The molecular evidence is sparse, with only three qPCR timepoints, and the model, while creative, rests on assumptions that are not yet fully supported by in vivo data.*

Please see our responses to the detailed comments.

> *Detailed comments are provided below:*
>
> *(1) The role for Orco proposed in the authors' model largely stems from the effects seen following the administration of (a single dose) of the Orco antagonist, OLC15. However, this hypothesis is undercut by the lack of adequate pharmacological controls, including a basic multipoint OLC15 dose-response series in addition to the administration of blockers for the other channels that are embedded in their model, but which were ruled out as being involved in the modulation of biological rhythms. In addition, these studies would (ideally) also benefit from the inclusion of the same concentration (series) of an inactive OLC15 analog to better control for off-target effects.*

The Orco agonist VUAA1 (Jones et al., 2011) binds directly to Orco and increases the channel open time probability. In *M. sexta* hawkmoths, we have already published that VUAA 1 increases the low spontaneous activity of ORNs in a dose-dependent fashion (Nolte et al., 2013). Chen and Luetje (2012) systematically varied the chemical structure of VUAA1 to identify new Orco ligands and discovered 22 Orco ligand candidates (OLCs) that either activated or inhibited Orco. In their heterologous expression system, Orco was most sensitive to inhibition by OLC15. Based on these results, we published a dose-response curve of OLC15 inhibition (1-100 µM) using *in vivo* tip recordings of pheromone-sensitive long trichoid sensilla of *M. sexta* (Nolte et al., 2016). There, we also demonstrated that OLC15 dose-dependently antagonizes the VUAA1-dependent activation of Orco.

Furthermore, we tested other published Orco antagonists, which were characterized in heterologous assays, in primary cell cultures of hawkmoth ORNs, as well as in *in vivo* assays

in intact hawkmoths. We focused on amiloride-derived antagonists, because we previously identified an amiloride-sensitive cation channel in hawkmoth ORNs. We found that, in contrast to OLC15, the amilorides HMA and MIA were not Orco-specific antagonists but instead affected different ion channel targets depending on the time of day (Nolte et al., 2016). Based on those experiments and the dose-response curves we determined that the Orco agonist VUAA1 (Jones et al., 2011) and the Orco antagonist OLC15 (Chen and Luetje, 2012) worked best in hawkmoth ORNs to target Orco pharmacologically. Due to those results and other comparative tests with other published Orco antagonists we settled since then in all further experiments on a dose of 50 µM OLC15 as most adequate to antagonize Orco functions in *Manudca*. In the current study, we focus on Orco without excluding the possibility that other ion channels in the ORNs contribute to the control of membrane potential rhythms.

We have clarified the Methods section accordingly.

> *(2) The expression pattern of Orco was assessed using qPCR at only three timepoints. Rhythmic transcripts can easily be missed with such sparse sampling (Hughes et al., 2017). A minimum of six evenly spaced timepoints across a 24-hour cycle would be required to confidently rule out circadian transcriptional regulation. In addition, the use of the timeless mRNA control from another study is not acceptable. Furthermore, qPCR analysis measures transcript abundance, not transcription, as the authors repeatedly state. Transcriptional studies would require nuclear run-off or, more recently, can be done with snRNAseq analysis. Taken together, these concerns undermine the authors' desire to rule out TTFL-based control that directly led them to implicate a PTTF-based model.*

We agree with the referees that more time points and a direct comparison between timeless and Orco mRNA levels should be included in this manuscript. We included these additional qPCR experiments and edited the manuscript to make clear that we measure transcript abundance, but we will not perform snRNAseq analysis due to time- and financial constraints.

> *(3) The modelling presented is based on Orco as a ZT-dependent conductance tied to the cAMP oscillations that were reported by this group in the cockroach and from the presence and functionality in Manduca of homomeric Orco complexes that are devoid of tuning ORs. While these complexes have been generated in cell culture and other heterologous expression systems, as well as presumably exist in vivo in the Drosophila empty neuron and other tuning OR mutants, there is no evidence that these complexes exist in wild-type Manduca ORNs. While this doesn't necessarily undermine every aspect of their models, the authors should note the presence of Orco/OR complexes rather than Orco homomeric complexes.*

Our ELISAs found circadian oscillations in cAMP levels not only in antennae of the Madeira cockroach (Schendzielorz et al., 2014, 2012), but also in hawkmoth antennae (Schendzielorz et al., 2015). For clarification, we added the 2015 citation to the Modeling chapter in the Methods section.

We agree with the referees that we cannot distinguish between Orco homo- and heteromers in the different compartments of our hawkmoth ORNs but we know that both are expressed in the pheromone-sensitive ORNs. Thus, as the referee suggests, we added text regarding the presence and localization of OR-Orco heteromers. Consistent data collected across different experiments (heterologous expression systems, primary cell cultures of hawkmoth ORNs, *in vivo*/*in situ* studies) support that Orco homomers are present in hawkmoth ORNs. In addition to co-expression of MsexOrco and MsexSNMP-1 with either MsexOr-1 or MsexOr-4 in a heterologous expression system, MsexOrco expression alone was already sufficient to increase intracellular Ca^{2+} levels spontaneously as a result of its property as leaky, non-

specific cation channel, and in response to VUAA1 application (Nolte et al., 2013). Both in developing hawkmoth pupae and differentiating primary cell cultures of hawkmoth ORNs, Orco expression started during a developmental time window where ORNs did not yet express pheromone receptors but where Orco affected spontaneous activity and intracellular Ca^{2+} levels dependent on VUAA1 (Nolte et al., 2016). *In vitro* patch clamp studies of differentiating cultured hawkmoth ORNs during this time window of pupal development characterized ion channels/currents with properties of Orco as a leaky, non-specific cation channel/current that depends on protein kinase C and cyclic nucleotides (Dolzer et al., 2021, 2008; Krannich and Stengl, 2008; Stengl, 1993). Thus, Orco homomers are present in developing hawkmoth ORNs during a time window where ORNs already express spontaneous activity but they do not heteromerize with pheromone receptors. However, we do not know whether and in what ratio homo- and heteromers of Orco and ORs are present in the respective sensillum compartments of adult hawkmoths because all OR-specific antibodies tested did not work in immunocytochemical studies of hawkmoth antennae (Nolte et al., 2013; Stengl, 1994; Stengl and Hildebrand, 1990). Our hypothesis of differential distribution of Orco homomers in the some and dendrite compartment, and OR-Orco heteromers in the cilia is based on differential immunocytochemical localization of *Drosophila* ORs mainly in the cilia compartment (Benton et al., 2006).

We clarified our manuscript accordingly.

> *(4) Some aspects of the authors' models, most notably the decision to phase align/optimize their DD and OLC15 recordings, are likely to bias their interpretations.*

It is consensus that insects display daily and circadian rhythms in pheromone-dependent mating, odor-gated feeding, and egg-laying behavior that phase-locks to environmental rhythms, corresponding with daily/circadian rhythms of sensory neuron physiology (e.g., Merlin et al., 2007; Rymer et al., 2007; Schendzielorz et al., 2015, 2012). However, circadian rhythms can be easily masked by stress, like the disturbances during an experimentally very challenging long-term recording experiment over several days. In addition, we observed over the years in our animal raising facility that in 17:7 light-dark cycles the originally nocturnal hawkmoths *M. sexta* distribute their activity patterns over the course of the day, finding nocturnal as well as diurnal hawkmoths. Thus, light-dark cycles were not enough to ensure phase-synchronized behavioral rhythms, and it is very likely that the nocturnal hawkmoths, next to stress signals, rely heavily on pheromone/odor dependent synchronization as also found in other moth species (Ghosh et al., 2024). Because we focus on spontaneous activity and not on pheromone-dependent physiology in this study, we used isolated males that were never exposed to the female pheromones, taking phase dispersal into account. Therefore, it became necessary in free-running conditions to first determine the respective behavioral rhythm for each animal, and then to phase-align their activity patterns to allow for statistical analysis. Otherwise, circadian differences would average out in a phase-dispersed free-running population. As requested by the referees in point (7), we added RAIN to test for rhythmicity in each of our recordings and revised the manuscript accordingly.

Furthermore, in preliminary experiments we briefly exposed hawkmoths to pheromone the night before the start of the experiment. However, we failed to obtain phase-synchronized spiking rhythms. Most likely, a circadian pattern of pheromone exposure would have been necessary as zeitgeber, which could not be used here due to long-term pheromone-dependent effects in spiking activity. These results are added as supplementary figure to Fig 3.

> *(5) The tip recordings from long trichoid sensilla are critical aspects of this study. These recordings were carried out on upper sensillar tips located on the distal-most second annulus. Since there are approximately 80 annuli on the Manduca antennae, it is unclear whether the recordings are representative of the antennal response.*

We think the reviewers might have misinterpreted our description of the recording site. In the Methods, we state that we clip off the 20 most distal annuli (leaving a stump of about 60 annuli) and insert the reference electrode into the flagellum up to the second annulus from the cut end, i.e., the recording sites are located at 2/3 – 3/4 of the antenna length as seen from the head of the animal. We clarified this in the Methods section.

In addition, our lab did show with antibody stainings against Orco that apparently all ORNs that innervate long and short trichoid sensilla along the whole flagellum express the same staining pattern (Nolte et al., 2016). Lee and Strausfeld (1990) mapped all types of antennal sensilla, and together with pheromone-dependent tip-recordings of Kaissling et al. (1989) it was shown that most of the male antennal sensilla are pheromone-sensitive long trichoid sensilla, with one of the two innervating ORNs always responding to bombykal, ensuring high sensitivity to pheromone detection. Furthermore, our patch clamp recordings of primary cell cultures of whole male antennae found largely overlapping ion channel populations across ORNs (review: (Stengl, 2010)). This would indicate that all ORNs, whether they express ORs sensitive to pheromone or general odorants, could potentially share the same Orco-dependent spontaneous activity rhythms. Furthermore, in our lab, different experimenters from different years that recorded from long trichoid sensilla on different annuli did not detect obvious differences in neither the spontaneous activity nor the pheromone responses (c.f., Dolzer et al., 2003; Gawalek and Stengl, 2018; Schneider et al., 2025). Thus, it is very likely that we are reporting a general encoding mechanism that is not locally restricted along the antennal flagellum and is very likely shared by all types of OR-Orco expressing ORNs.

> *(6.1) The authors do not provide any data in support of their cAMP/cGMP-based Orco gating…*

There are publications supporting cyclic nucleotide gating of Orco in *Drosophila*, but only after previous phosphorylation via protein kinase C (PKC; review: (Wicher and Miazzi, 2021)). Since Orco is very conserved among insect species, it is likely that PKC- and cGMP/cAMP-dependent regulations are present for Orco in other insect species. To test this, we are currently characterizing second messenger-dependence of spontaneous spiking activity, which is the focus of a follow-up manuscript. Nevertheless, to provide more evidence for our hypothesis of the current manuscript, we added a new set of tip-recording experiments that demonstrate cAMP-dependent gating of Orco. Because of the addition of this figure, we merged figures 8-10 into Figure 8 and added the cAMP data as Figure 9.

> *(6.2) … and the PTTF model proposed is somewhat disappointing.*

For a detailed introduction of our PTFL membrane clock hypothesis please see our opinion paper that we refer to in the manuscript (Stengl and Schneider, 2024). We added clarification of how Orco activation can influence cAMP levels. A more elaborate PTFL clock model including many more of the identified ion channels in hawkmoth ORNs is the focus of another manuscript to come.

> *(6.3) The model seems to be influenced by their long-held proposal that insect olfactory signaling has a critical metabotropic component involving cyclic nucleotides, PKC, etc, a view that may be influenced by the use of Orco homomeric complexes generated in HEK cells.*

Indeed, we propose a metabotropic pheromone-transduction cascade, which in moths and cockroaches is based on G-protein-mediated activation of phospholipase C but not on adenylyl cyclase activation. Our hypothesis is not influenced by HEK cell heterologous expression studies of Orco but is supported by our own work comparing *in vivo* tip recordings of intact hawkmoths with patch clamp experiments on hawkmoth primary cell cultures of olfactory receptor neurons, which are able to respond to their species-specific pheromones *in vitro*

(Schneider et al., 2025; Stengl, 2010; Stengl and Funk, 2013; Wicher and Miazzi, 2021). In addition, a multitude of publications by other laboratories with *in vivo* and *in vitro* studies using physiological, genetic, and immunocytochemical assays all support a metabotropic signal transduction cascade in insect olfaction (Stengl, 2010; Stengl and Funk, 2013; Takagi et al., 2025; Wicher and Miazzi, 2021). In contrast, the hypothesis suggesting a solely ionotropic pheromone- and general odor-dependent transduction cascade for all insect species is based on very sparse experimental evidence, based primarily on heterologous expression studies such as HEK cells that lack the insect's WT molecular surroundings, and thus, cannot predict OR-Orco function *in vivo*. Furthermore, the ionotropic hypothesis is heavily based upon the argument that an inverse 7TM receptor cannot couple to G-proteins, which lacks careful backup via biochemical and structural studies. In addition, the ionotropic hypothesis lacks support via carefully performed physiological *in vivo* studies in different insect species that paid attention to analysis of the distinct kinetic components of ORNś odor/pheromone responses and that employ physiological concentrations and durations of odor/pheromone stimuli (please see our most recent publication by Schneider et al. (2025)). We added references to the possible odor transduction mechanisms to the introduction.

> *(6.4) Nevertheless, structural studies on Orco do not support a cyclic nucleotide binding site, although PKC-based phosphorylation has been implicated in the fine-tuning/adaptation of olfactory signaling.*

While structural studies did not find evidence for conserved known cyclic nucleotide binding sites on Orco, this does not exclude the presence of indirect cAMP effects via e.g., Orco subunits complexing with other molecules under direct cAMP control, such as other ion channel subunits. Furthermore, it does not exclude so far unknown binding sites, or via sites that fold out only after a specific sequence of previous phosphorylations of the many phosphorylation sites on Orco. Indeed, physiological studies in *Drosophila* presented evidence for cyclic nucleotide dependence of Orco after previous PKC-dependent phosphorylation (Getahun et al., 2013). Our ongoing *in vivo* experiments in hawkmoths further corroborate a zeitgeber time-dependent PKC- and cyclic nucleotide-dependent modulation of Orco. These detailed studies will be published in a follow-up publication. In the revised version of this manuscript, we added tip-recording experiments that indicate cAMP involvement in Orco gating (new Figure 9).

> *(7) Because only 5/11 LD and 7/10 DD animals showed daily rhythms, with averages lacking clear daily modulation, the methods are not sufficiently reliable enough to reveal novel underlying mechanisms of circadian rhythm generation. The reported results are therefore not yet reliable or quantifiable. To quantify their results, the authors should apply tests for circadian rhythmicity using methods such as RAIN, JTK CYCLE, MetaCycle, or Echo. The use of FFT and Wavelet is applauded, but these methods do not have tests of significance for rhythms and can be biased when analyzing data in which there could only be 1-3 circadian cycles. Because the conclusions appear to be based on 11-12 neurons that were recorded for 2-4 days, the reader is concerned that the methods are not yet perfected to provide strong evidence for circadian regulation of spontaneous firing of ORNs. The average data (e.g., Figure 3Bii and 3Cii) highlight the apparent lack of daily rhythms. In summary, the results would be more compelling if more than 50% of the recordings had significant circadian amplitudes and with similar periods and phases.*

The long-term tip-recordings of intact hawkmoths are very challenging and take a very long time to accomplish, thus, we are very happy that we succeeded in obtaining so many of them (N=40). We are thankful to the reviewers' suggestion to use RAIN since this analysis revealed circadian rhythms in 7 of 11 LD recordings, 8 of 12 DD recordings, and 2 of 12 OLC15 recordings. Please see also our response to (4) above, commenting the phase-dispersal of activity rhythms observed in our experiments, as well as in the behavior of hawkmoth males in the mating cage.

> *(8) The statement that circadian patterns of ORN firing are lost with the Orco antagonist (OLC15) is not strongly supported. The manuscript should be revised to quantify how Orco changed circadian amplitude in the 12 recorded neurons. Measures of circadian amplitude can avoid confusing/vague statements like Line 394 "low and high frequency bands appeared to merge during the activity phase around ZT 0 in the animals that showed clear circadian rhythms (N = 5 of 11 in LD)". The conclusion that Orco blocks circadian firing appears to be contradicted by Figure 6, which indicates that ~6 of these neurons had circadian periods detected by wavelet. The manuscript would be strengthened with details about the specificity and reproducibility of the Orco antagonist. The authors quantify the gradual decrease in firing with the slope of a linear fit to estimate how the "effectiveness [of OLC15] increased over time." They conclude that the drug "obliterated circadian rhythms and attenuated the spontaneous activity in several, but not all experiments (N = 8 of 12)." The report would be greatly strengthened with corroborating data from additional Orco antagonists and additional doses of OLC15 (the authors use only 50 uM OLC15).*

According to the valuable suggestions of the referees, we used RAIN to detect circadian rhythms in the spiking attributes in each individual animal. Since only 2 of 12 animals displayed a circadian rhythm in OLC15, statistical comparison of circadian amplitudes is not possible. We revised the results section accordingly and added to the figure legend to make it clearer that the heat maps in Fig 5 are representative from one animal each and not averages across animals.

As the reviewer states correctly in (7), wavelet results of circadian rhythmicity must be interpreted carefully because of the low number of circadian cycles in ~3-4 day recordings. Since the heatmaps in Figure 5 visually revealed the presence of ultradian rhythms, the main focus of the wavelet analysis in Figure 6 is in the detection and quantification of ultradian periods up to 20 h.

We revised the Methods section to include references to previous experiments that characterized the effect of different doses of OLC15 and other Orco antagonists and agonists in *M. sexta* antennae (Nolte et al., 2016). Please see also our response to (1).

> *(9) The manuscript includes several statements that are more speculation than conclusion. For example, there is no evidence for tuning or plasticity in this report. Statements like the following should be removed or addressed with experiments that show changes in odor response specificity or sensitivity: "ORN signalosomes are highly plastic endogenous PTFL clocks comprising receptors for circadian and ultradian Zeitgebers that allow to tune into internal physiological and external environmental rhythms as basis for active sensing." (Discussion Line 622). The paper concludes that (line 380) "mean frequency of spontaneous spiking and the frequency of bursting expressed daily modulation, and are both most likely controlled via a circadian clock that targets the leak channel Orco." This is too bold given the available results.*

We revised the manuscript accordingly and clarified which statements are supported via published evidence and which are predictions based upon our novel hypothesis published in our opinion paper (Stengl and Schneider, 2024).

> *(10.1) Because Orco conductance is modulated by cyclic nucleotides, it remains highly plausible that circadian regulation occurs upstream at the level of signaling pathways (e.g., calcium, calcium-binding proteins, GPCRs, cyclases, phosphodiesterases).*

We agree with the referees that it is very likely that there are multiple layers of interconnected feedback cycles that control Orco localization and activity. Our novel hypothesis suggests interlocked TTFL and PTFL control of physiological circadian rhythms,

not strictly hierarchical TTFL control, which would require a daily turnover of membrane proteins and transcriptional control via the established TTFL clock in insect ORNs. We are currently searching for TTFL control at all levels of odor/pheromone transduction using ZT-dependent transcriptomics in combination with qPCR and single-nucleus transcriptomics, involving also all the molecules suggested by the referees. These studies are ongoing, are very time- and money-consuming, and are beyond the scope of this manuscript. However, we added a set of experiments to this manuscript in which we demonstrate that the effect of increased cAMP on the spontaneous spiking activity is mediated by Orco (new Figure 9).

> *(10.2) The possibility that circadian oscillations of cyclic nucleotides are generated by the canonical TTFL mechanism has not been excluded. In fact, extensive work in Drosophila has demonstrated that the TTFL-based molecular clock proteins are required for circadian rhythms in olfaction.*

Our experiments that test circadian TTFL control at different levels of the cAMP transduction cascade in hawkmoth antennae are on the way and are part of another publication. In section 6.2 we already stated that our experiments do not exclude that Orco is under indirect control of the TTFL. We revised our discussion accordingly.

The experiments published for TTFL dependent control of *Drosophila* olfaction that we are aware of (Krishnan et al., 1999; Tanoue et al., 2004) do not exclude interlinked PTFL and TTFL clocks. Krishnan et al. (1999) demonstrated that the TTFL clock in antennal olfactory receptor neurons correlates with circadian rhythms in odor responses measured in electroantennogram (EAG) recordings, not in single sensillum recordings as in our experiments. EAG recordings comprise not only voltage responses of the olfactory sensory neurons but also voltage changes generated in non-neuronal antennal cells such as trichogen and tormogen cells that built the transepithelial potential gradient via vATPases that generates the high K^+ concentration in the sensillum lymph (Jain et al., 2024; Klein, 1992; Thurm and Küppers, 1980). In addition, EAG recordings most likely contain responses of afferent neurons originating from somata in the brain that maintain central control of the antennae. Thus, EAG recordings are difficult to interpret.

> *(11) A defining feature of circadian oscillators is the feedback mechanism that generates a time delay (e.g., PERIOD/TIMELESS repressing their own transcription). While the authors describe how cyclic nucleotides can regulate Orco conductance, they do not provide a convincing explanation of how Orco activity could, in turn, feed back into the proposed PTFL to sustain oscillations. For these reasons, the authors should consider:*
>
> *(a) Providing a broader discussion of non-TTFL models of circadian rhythms (e.g., redox cycles, post-translational modifications).*

We revised the discussion accordingly.

> *(b) Reassessing Orco expression using a higher-resolution temporal sampling ({greater than or equal to}6 timepoints per 24 h).*

We added those experiments to the revised version of the manuscript (see our response to (2)).

> *(c) Clarifying or revising the PTFL model to explicitly address how feedback would be achieved. Alternatively, the data may be more consistent with Orco conductance rhythms being regulated by post-translational mechanisms downstream of the canonical TTFL oscillator, as suggested by the Drosophila olfactory system literature.*

We added possible negative feedback elements to the Discussion to explain how our proposed PTFL could in principle work independent of TTFL clock.

> *Minor weaknesses:*
>
> *(1) The authors should compare the firing patterns of ORN neurons to the bursts, clusters, and packets of retinal efferent spikes reported in Liu JS and Passaglia CL (2011; JBR). By comparing measures in moths to measures in Limulus, the authors might be able to address the question: Is the daily firing pattern of ORN neurons likely a conserved feature of circadian control of sensory sensitivity?*

We have revised the discussion accordingly.

> *(2) The methods need further details. For example, it is unclear if or how single neuron activity was discriminated and whether the results were compromised by the relatively large environmental fluctuations in temperature (21-27oC), humidity (35-60%), or other cues known to modulate spontaneous firing.*

These large fluctuations stem from doing experiments at different seasons (higher temperature and humidity in the summer months, lower temperature and humidity in winter). Throughout each individual experiment, conditions were stable. We clarified the Methods section accordingly.

> ***Recommendations for the authors:***
>
> *The authors should post the code for their computational model to a repository like GitHub.*

The code for the computational model is now available at *https://github.com/a-c-schneider/VijayanForlinoEtAl2025_Model.git*

References

Benton R, Sachse S, Michnick SW, Vosshall LB. 2006. Atypical Membrane Topology and Heteromeric Function of Drosophila Odorant Receptors In Vivo. PLOS Biology 4:e20. DOI: *https://doi.org/10.1371/journal.pbio.0040020*

Chen S, Luetje CW. 2012. Identification of New Agonists and Antagonists of the Insect Odorant Receptor Co-Receptor Subunit. PLOS ONE 7:e36784. DOI: *https://doi.org/10.1371/journal.pone.0036784*

Dolzer J, Fischer K, Stengl M. 2003. Adaptation in pheromone-sensitive trichoid sensilla of the hawkmoth Manduca sexta. Journal of Experimental Biology 206:1575–1588. DOI: *https://doi.org/10.1242/jeb.00302*

Dolzer J, Krannich S, Stengl M. 2008. Pharmacological Investigation of Protein Kinase C- and cGMP-Dependent Ion Channels in Cultured Olfactory Receptor Neurons of the Hawkmoth Manduca sexta. Chemical Senses 33:803–813. DOI: *https://doi.org/10.1093/chemse/bjn043*

Dolzer J, Schröder K, Stengl M. 2021. Cyclic nucleotide-dependent ionic currents in olfactory receptor neurons of the hawkmoth Manduca sexta suggest pull–push sensitivity modulation. European Journal of Neuroscience 54:4804–4826. DOI: *https://doi.org/10.1111/ejn.15346*

Gawalek P, Stengl M. 2018. The Diacylglycerol Analogs OAG and DOG Differentially Affect Primary Events of Pheromone Transduction in the Hawkmoth Manduca sexta in a Zeitgebertime-Dependent Manner Apparently Targeting TRP Channels. Frontiers in Cellular Neuroscience 12:218. DOI: *https://doi.org/10.3389/fncel.2018.00218*

Getahun MN, Olsson SB, Lavista-Llanos S, Hansson BS, Wicher D. 2013. Insect Odorant Response Sensitivity Is Tuned by Metabotropically Autoregulated Olfactory Receptors. PLOS ONE 8:e58889. DOI: *https://doi.org/10.1371/journal.pone.0058889*

Ghosh S, Suray C, Bozzolan F, Palazzo A, Monsempès C, Lecouvreur F, Chatterjee A. 2024. Pheromone-mediated command from the female to male clock induces and synchronizes circadian rhythms of the moth Spodoptera littoralis. Current biology 34:1414-1425.e5. DOI: *https://doi.org/10.1016/j.cub.2024.02.042*, PMID: 38479388

Jain K, Prelic S, Hansson BS, Wicher D. 2024. Expression of Drosophila melanogaster V-ATPases in Olfactory Sensillum Support Cells. Insects 15:1016. DOI: *https://doi.org/10.3390/insects15121016*

Jones PL, Pask GM, Rinker DC, Zwiebel LJ. 2011. Functional agonism of insect odorant receptor ion channels. Proceedings of the National Academy of Sciences 108:8821–8825. DOI: *https://doi.org/10.1073/pnas.1102425108*

Kaissling KE, Hildebrand JG, Tumlinson JH. 1989. Pheromone receptor cells in the male moth Manduca sexta. Archives of Insect Biochemistry and Physiology 10:273–279. DOI: *https://doi.org/10.1002/arch.940100403*

Klein U. 1992. The insect V-ATPase, a plasma membrane proton pump energizing secondary active transport: immunological evidence for the occurrence of a V-ATPase in insect ion-transporting epithelia. Journal of Experimental Biology 172:345–354. DOI: *https://doi.org/10.1242/jeb.172.1.345*

Krannich S, Stengl M. 2008. Cyclic Nucleotide-Activated Currents in Cultured Olfactory Receptor Neurons of the Hawkmoth Manduca sexta. Journal of Neurophysiology 100:2866–2877. DOI: *https://doi.org/10.1152/jn.01400.2007*

Krishnan B, Dryer SE, Hardin PE. 1999. Circadian rhythms in olfactory responses of Drosophila melanogaster. Nature 400:375–378. DOI: *https://doi.org/10.1038/22566*

Lee JK, Strausfeld NJ. 1990. Structure, distribution and number of surface sensilla and their receptor cells on the olfactory appendage of the male mothManduca sexta. Journal of Neurocytology 19:519–538. DOI: *https://doi.org/10.1007/BF01257241*

Merlin C, Lucas P, Rochat D, François M-C, Maïbèche-Coisne M, Jacquin-Joly E. 2007. An Antennal Circadian Clock and Circadian Rhythms in Peripheral Pheromone Reception in the Moth Spodoptera littoralis. Journal of Biological Rhythms 22:502–514. DOI: *https://doi.org/10.1177/0748730407307737*

Nolte A, Funk NW, Mukunda L, Gawalek P, Werckenthin A, Hansson BS, Wicher D, Stengl M. 2013. In situ Tip-Recordings Found No Evidence for an Orco-Based Ionotropic Mechanism of Pheromone-Transduction in Manduca sexta. PLOS ONE 8:e62648. DOI: *https://doi.org/10.1371/journal.pone.0062648*

Nolte A, Gawalek P, Koerte S, Wei H, Schumann R, Werckenthin A, Krieger J, Stengl M. 2016. No Evidence for Ionotropic Pheromone Transduction in the Hawkmoth Manduca sexta. PLOS ONE 11:e0166060. DOI: *https://doi.org/10.1371/journal.pone.0166060*

Rymer J, Bauernfeind AL, Brown S, Page TL. 2007. Circadian rhythms in the mating behavior of the cockroach, Leucophaea maderae. Journal of Biological Rhythms 22:43–57. DOI: *https://doi.org/10.1177/0748730406295462*, PMID: 17229924

Schendzielorz J, Schendzielorz T, Arendt A, Stengl M. 2014. Bimodal Oscillations of Cyclic Nucleotide Concentrations in the Circadian System of the Madeira Cockroach Rhyparobia maderae. Journal of Biological Rhythms 29:318–331. DOI: *https://doi.org/10.1177/0748730414546133*

Schendzielorz T, Peters W, Boekhoff I, Stengl M. 2012. Time of Day Changes in Cyclic Nucleotides Are Modified via Octopamine and Pheromone in Antennae of the Madeira Cockroach. Journal of Biological Rhythms 27:388–397. DOI: *https://doi.org/10.1177/0748730412456265*

Schendzielorz T, Schirmer K, Stolte P, Stengl M. 2015. Octopamine Regulates Antennal Sensory Neurons via Daytime-Dependent Changes in cAMP and IP3 Levels in the Hawkmoth Manduca sexta. PLOS ONE 10:e0121230. DOI: *https://doi.org/10.1371/journal.pone.0121230*

Schneider AC, Schröder K, Chang Y, Nolte A, Gawalek P, Stengl M. 2025. Hawkmoth Pheromone Transduction Involves G-Protein–Dependent Phospholipase Cβ Signaling. eNeuro 12:ENEURO.0376-24.2024. DOI: *https://doi.org/10.1523/ENEURO.0376-24.2024*, PMID: 39880675

Stengl M. 2010. Pheromone Transduction in Moths. Frontiers in Cellular Neuroscience 4:133. DOI: *https://doi.org/10.3389/fncel.2010.00133*

Stengl M. 1994. Inositol-trisphosphate-dependent calcium currents precede cation currents in insect olfactory receptor neurons in vitro. Journal of Comparative Physiology A 174:187–194. DOI: *https://doi.org/10.1007/BF00193785*

Stengl M. 1993. Intracellular-Messenger-Mediated Cation Channels in Cultured Olfactory Receptor Neurons. Journal of Experimental Biology 178:125–147. DOI: *https://doi.org/10.1242/jeb.178.1.125*

Stengl M, Funk NW. 2013. The role of the coreceptor Orco in insect olfactory transduction. Journal of Comparative Physiology A 199:897–909. DOI: *https://doi.org/10.1007/s00359-013-0837-3*

Stengl M, Hildebrand JG. 1990. Insect olfactory neurons in vitro: morphological and immunocytochemical characterization of male-specific antennal receptor cells from developing antennae of male Manduca sexta. Journal of Neuroscience 10:837–847. DOI: *https://doi.org/10.1523/JNEUROSCI.10-03-00837.1990*, PMID: 2319305

Stengl M, Schneider AC. 2024. Contribution of membrane-associated oscillators to biological timing at different timescales. Frontiers in Physiology 14:1243455. DOI: *https://doi.org/10.3389/fphys.2023.1243455*

Takagi S, Abuin L, Mermet J, Lee D, Benton R. 2025. A GPCR signaling pathway in insect odor detection. DOI: *https://doi.org/10.1101/2025.10.03.680299*

Tanoue S, Krishnan P, Krishnan B, Dryer SE, Hardin PE. 2004. Circadian Clocks in Antennal Neurons Are Necessary and Sufficient for Olfaction Rhythms in Drosophila. Current Biology 14:638–649. DOI: *https://doi.org/10.1016/j.cub.2004.04.009*, PMID: 15084278

Thurm U, Küppers J. 1980. Epithelial physiology of insect sensilla. In: Locke M, Smith DS (Eds). Insect Biology in the Future. Academic Press. p. 735–763. DOI: *https://doi.org/10.1016/B978-0-12-454340-9.50039-2*

Wicher D, Miazzi F. 2021. Functional properties of insect olfactory receptors: ionotropic receptors and odorant receptors. Cell and Tissue Research 383:7–19. DOI: *https://doi.org/10.1007/s00441-020-03363-x*

https://doi.org/10.7554/eLife.108100.2.sa0